

**ISTANBUL TECHNICAL UNIVERSITY ★ ENERGY INSTITUTE**

**A STUDY OF THE DEPENDENCE OF SOURCE EFFICIENCY ON DESIGN  
PARAMETERS IN SOURCE-DRIVEN SUBCRITICAL NUCLEAR SYSTEMS**

**M.Sc. THESIS**

**Ceyhun YAVUZ**

**(301091093)**

**Program:Energy Science and Technology**

**Division:Nuclear Researches**

**Thesis Advisor: Prof. Dr. Atilla ÖZGENER**

**JANUARY 2015**



**ISTANBUL TECHNICAL UNIVERSITY ★ ENERGY INSTITUTE**

**A STUDY OF THE DEPENDENCE OF SOURCE EFFICIENCY ON DESIGN  
PARAMETERS IN SOURCE-DRIVEN SUBCRITICAL NUCLEAR SYSTEMS**

**M.Sc. THESIS**

**Ceyhun YAVUZ  
(301091093)**

**Program:Energy Science and Technology**

**Division:Nuclear Researches**

**Thesis Advisor: Prof. Dr. Atilla ÖZGENER**

**JANUARY 2015**



**İSTANBUL TEKNİK ÜNİVERSİTESİ ★ ENERJİ ENSTİTÜSÜ**

**KAYNAK GÜDÜMLÜ ALT KRİTİK SİSTEMLERDE KAYNAK  
VERİMLİLİĞİNİN DİZAYN PARAMETRELERİNE BAĞIMLILIĞININ  
İNCELENMESİ**

**YÜKSEK LİSANS TEZİ**

**Ceyhun YAVUZ  
(301091093)**

**Program: Enerji Bilimleri ve Teknolojileri**

**Anabilim Dalı: Nükleer Araştırmalar**

**Tez Danışmanı: Prof. Dr. Atilla ÖZGENER**

**OCAK 2015**



**Ceyhun Yavuz**, a **M.Sc.** student of **ITU Graduate School of Energy** student ID **301091093**, successfully defended the **thesis/dissertation** entitled “**A STUDY OF THE DEPENDENCE OF SOURCE EFFICIENCY ON DESIGN PARAMERTERS IN SOURCE-DRIVEN SUBCRITICAL NUCLEAR SYSTEMS**”, which he prepared after fulfilling the requirements specified in the associated legislations, before the jury whose signatures are below.

**Thesis Advisor :**      **Prof. Dr. Atilla ÖZGENER**      .....

Istanbul Technical University

**Jury Members :**      **Prof. Dr. Atilla Özgener**      .....

Istanbul Technical University

**Prof. Dr. Serhat Şeker**      .....

Istanbul Technical University

**Prof. Dr. Tayfun Büke**      .....

Muğla Sıtkı Koçaman University

**Date of Submission : 15 December 2014**

**Date of Defense : 21 January 2015**





*To my sister, family and ever beloved Berna Yalızay*



## **FOREWORD**

I would like to thank and express gratitude to my thesis professor Prof.Dr.Atilla Özgener and Prof.Dr.Bilge Özgener, from whom I have learned about nuclear energy science, for supporting and guiding me through this thesis.

December 2014

Ceyhun YAVUZ  
Physics Engineer



## TABLE OF CONTENTS

	<u>Page</u>
<b>FOREWORD</b> .....	v
<b>TABLE OF CONTENTS</b> .....	vii
<b>ABBREVIATIONS</b> .....	x
<b>LIST OF TABLES</b> .....	xii
<b>LIST OF FIGURES</b> .....	xiv
<b>SUMMARY</b> .....	xvi
<b>ÖZET</b> .....	xviii
<b>1. INTRODUCTION</b> .....	1
<b>2. A BRIEF REVIEW OF THE BASICS OF ACCELERATOR DRIVEN SYSTEMS</b> .....	5
2.1 Transmutation of Actinides for Solution of the Nuclear Waste Problem .....	5
2.2 Components of Accelerator Driven Systems .....	6
2.2.1 Proton accelerator .....	6
2.2.1.1 Linear accelerators .....	7
2.2.1.2 Cyclotron accelerators.....	7
2.2.2 Spallation target .....	7
2.2.3 Fuel elements .....	8
2.2.3.1 Oxide fuels .....	8
2.2.3.2 Nitride fuels.....	9
2.2.3.3 Metal fuels.....	9
2.2.4 Coolant .....	9
2.2.4.1 Lead or lead-bismuth eutectic .....	10
2.2.4.2 Sodium .....	10
2.2.4.3 Gas .....	10
<b>3. SOURCE MULTIPLICATION , SUBCRITICAL MULTIPLICATION FACTOR AND SOURCE EFFICIENCY</b> .....	13
3.1 Neutron Importance Function .....	13
3.2 Source Multiplication and Reactor Power .....	14
3.3 Subcritical Multiplication Factor .....	16
3.4 Source Efficiency .....	16
<b>4. BENCHMARK ANALYTICAL SOLUTIONS</b> .....	19
4.1 One Group One Region Flat Source .....	19
4.2 One Group One Region Dirac Source.....	25
4.3 One Group Two Region System with Flat Source in the Inner Region.....	32
4.4 Two Group One Region Dirac Source .....	38
<b>5. MATHEMATICA MODELS FOR BENCHMARK SOLUTIONS</b> .....	47
5.1 One Group One Region Flat Source .....	47
5.2 One Group One Region Dirac Source.....	48
5.3 One Group Two Region System With Flat Source In the Inner Region.....	49
5.4 Two Group One Region Dirac Source .....	51

<b>6. COMPARISON OF ANALYTICAL AND NUMERICAL RESULTS.....</b>	<b>55</b>
6.1 One Group One Region Flat Source .....	55
6.2 One Group One Region Dirac Source.....	55
6.3 One Group Two Region System with Flat Source in the Inner Region.....	56
6.4 Two Group One Region Dirac Source .....	57
<b>7. SOURCE EFFICIENCY .....</b>	<b>59</b>
7.1 Target Radius and Source Efficiency.....	59
7.2 Blanket Radius and Source Efficiency.....	62
7.3 Am-Pu Ratio Comparisons for An ADS .....	63
<b>8. CONCLUSION.....</b>	<b>69</b>
<b>REFERENCES .....</b>	<b>71</b>
<b>CURRICULUM VITAE.....</b>	<b>73</b>



## **ABBREVIATIONS**

<b>ADS</b>	: Accelerator Driven System
<b>LDE</b>	: Lead Bismuth Eutectic
<b>MA</b>	: Minor Actinides
<b>RF</b>	: Radio Frequency





## LIST OF TABLES

	<u>Page</u>
<b>Table 2.1</b> : Physical properties of the main liquid metal coolant options (Per Seltborg, 2005).....	10
<b>Table 6.1</b> : One Group One Region Flat Source Numerical Analytical Comparison .....	55
<b>Table 6.2</b> : One Group One Region Dirac Source Numerical Analytical Comparison .....	56
<b>Table 6.3</b> : One Group Two Region with Flat Source in the First Region Numerical Analytical Comparison.....	57
<b>Table 6.4</b> : Two Group One Region Dirac Source In the First Region Numerical Analytical Comparison.....	58
<b>Table 6.4</b> : Two Group One Region Dirac Source In the First Region Numerical Analytical Comparison.....	58
<b>Table 7.1</b> : Nuclear Parameters for 7.Source Efficiency .....	59
<b>Table 7.2</b> : Target Radius and Source Efficiency Comparison .....	60
<b>Table 7.3</b> : Blanket Radius and Source Efficiency Comparison .....	62
<b>Table 7.4</b> : Elemental Densities.....	63
<b>Table 7.5</b> : Isotopic Compositions.....	64
<b>Table 7.6</b> : Elemental Atom Densities.....	65
<b>Table 7.7</b> : Elemental One Group Cross Sections .....	65
<b>Table 7.8</b> : Target and Fuel Cross Sections.....	66
<b>Table 7.9</b> : Nuclear Parameters for Pu/Am Mix Percentages.....	67



## LIST OF FIGURES

	<u>Page</u>
<b>Figure 2.1</b> : Variation of Radiotoxic Inventory with Respect to Time in Discharged Fuel. ....	5
<b>Figure 2.2</b> : Half-lives of Actinides and Fission Products. ....	6
<b>Figure 2.3</b> : Components of an ADS. ....	6
<b>Figure 5.1</b> : One group one region flat source change of $keff$ and $ks$ with $x$ .....	47
<b>Figure 5.2</b> : One group one region flat source change of $Ms$ with $x$ . ....	47
<b>Figure 5.3</b> : One group one region flat source change of $\varphi *$ with $x$ .....	48
<b>Figure 5.4</b> : One group one region Dirac source change of $keff$ and $ks$ with $x$ ....	48
<b>Figure 5.5</b> : One group one region Dirac source change of $Ms$ with $x$ .....	49
<b>Figure 5.6</b> : One group one region Dirac source change of $\varphi *$ with $y$ .....	49
<b>Figure 5.7</b> : One group two region with flat source in the first region change of $keff$ and $ks$ with $R_0$ .....	50
<b>Figure 5.8</b> : One group two region with flat source in the first region change of $Ms$ with $R_0$ .....	50
<b>Figure 5.9</b> : One group two region with flat source in the first region change of $\varphi *$ with $R_0$ .....	51
<b>Figure 5.10</b> : Two group one region Dirac source change of $keff, tks$ and $ks$ with $R_0$ .....	51
<b>Figure 5.11</b> : Two group one region Dirac source change of $Ms, tMs$ with $R_0$ ....	52
<b>Figure 5.12</b> : Two group one region Dirac source region change of $tks, ks$ with source position $r_0$ .....	52
<b>Figure 5.13</b> : Two group one region Dirac source region change of $\varphi *, t\varphi *$ .....	53
<b>Figure 7.1</b> : Target Radius and Source Efficiency Comparison.....	62
<b>Figure 7.2</b> : Blanket Radius and Source Efficiency Comparison.....	63
<b>Figure 7.3</b> : $k_s$ vs plutonium weight percentage in Pu Am Fuel.....	67
<b>Figure 7.4</b> : $\varphi *$ vs plutonium weight percentage in Pu Am Fuel .....	68



# **A STUDY OF THE DEPENDENCE OF SOURCE EFFICIENCY ON DESIGN PARAMETERS IN SOURCE-DRIVEN SUBCRITICAL NUCLEAR SYSTEMS**

## **SUMMARY**

ADS, which is first proposed by Carlo Rubbia, is an operationally safe alternative for incineration, transmutation since it has a sub critical core and with a fast neutron Unified with a power production perspective, source efficiency presents a paramount importance. The major energy input in an ADS design, is the accelerator power. With increased source efficiency, it is possible to minimize this energy and maximize productivity.

In this thesis, first a brief introduction to ADS is provided. In some, detail the transmutation concept, accelerators, spallation targets, fuel elements and coolant are discussed.

Following that the theory of source multiplication, subcritical multiplication factor and source efficiency are presented, since these concepts are crucial to ADS design. Four benchmark analytical solutions in spherical coordinates were presented as: “One Group One Region Flat Source”, “One Group One Region Dirac Source”, “One Group Two Region System with Flat Source in the Inner Region”, “Two Group One Region Dirac Source”.

The behaviors of key parameters were studied for the four benchmark solutions through Mathematica modelled graphs.

Then, using finite difference multi group diffusion code DIFSP, the analytical results and numerical result are compared for the four benchmark solutions and the calculated nuclear parameters associated error margins are presented.

Concluding the authenticity of solutions, the variations of source efficiency with respect to ADS parameters is assessed. Tables and figures for target radius and source efficiency, blanket radius and source efficiency are presented and their relations are discussed.

Also parameters for an alternative fuel option of ADS, americium and plutonium mix, are calculated and discussed for different ratios, acting as a benchmark for minor Actinide fuels.

Lastly, a brief summary of the results and inferences for ADS are presented.



# KAYNAKLA SÜRÜLEN ALT KRİTİK SİSTEMLERDE KAYNAK VERİMLİLİĞİNİN DİZAYN PARAMETRELERİNE BAĞIMLILIĞININ İNCELENMESİ

## ÖZET

Temelde klasik nükleer üretim süreçlerinde, fisil çekirdeğin parçalanması ile ortaya çıkan fisyon ürünleri ve nötron ilgili çekirdek tarafından yutulduğu zaman oluşan transuranyum malzemeler, saniyeler mertebesinde yüz bin yıllara uzanan yarı ömürlü aktif çekirdeklerin oluşmasına yol açarlar.

Nükleer endüstrinin, atık yakıtlardan plutonyum ve uranyumu ayrıştırmak için kullandığı PUREX süreçleri olsa da, bunun dışında minör aktinidlere dair bir süreçleri olmaması sebebi ile, geri kalan atık için takip edilen yöntem, uzun zamanlı gömme yöntemidir.

Hem yüksek seviyeli radyasyon kirliliği hem de yarı ömürlenme zamanlarının ciddi şekilde uzun olması, bu metod üzerinde güvenlik ve finansal anlamda baskı yaratmaktadır.

Bu aktif çekirdeklerin bir çoğu için daha nötron yutma yolu ile daha stabil bir çekirdek haline dönüştürülmesi veya fisyonu uğratılması mümkündür. Özellikle uranyum ötesi malzemelerin fisyonu uğraması ile zaman baskısının ciddi şekilde azaltılabileceği değerlendirilmiştir.

Bu bakış açısında hareketle Carlo Rubbia, kaynak tahrikli alt kritik sistem fikrini öne sürmüştür. Temelde, plutonyum ve minör aktinidlerin yüksek fisyon tesir kesitinden hareketle, hızlı reaktör olarak tasarlanmış bu sistem, operasyonun güvenliğine binaen de, alt kritik bir dizayna, yani öz sistemin bir nötron başına birden az nötron ürettiği bir içeriğe sahiptir. Sistemin sönmemesi ve reaksiyonun devamı için, dışarıdan proton hızlandırıcı tarafından dövülen bir kaynaktan (ör: kurşun) türeyen kaynak nötronları, sisteme aktarılır. Tasarım, bu yol ile, hem yarı ömrü çok uzun olan atıkların, daha kabul edilebilir yarı ömürlü çekirdeklere dönüşmesini, hem de enerji üretimini hedeflemektedir.

Ancak ilgili dizaynın verimli bir şekilde çalışması, temelde hızlandırıcının harcadığı enerjinin minimize edilmesi ve bu paralelde enerji üretiminin maksimize edilmesi ile mümkündür. Temelde üretilen kaynak nötronu başına üretilen enerjinin maksimize edilmesi gerekmektedir. Kaynak verimliliği bu anlamda, tezin temel konusudur ve dizaynın ana parametresidir.

Her şeyden önce kaynak tahrikli alt kritik sistemler ile ilgili temel bilgiler ifade edilmiştir. Bir ADS'nin, temel bileşenleri olarak; yakıt, hedef, hızlandırıcı ve soğutucu bu tez kapsamında incelenmiştir.

Yakıtlar için oksit, metal ve nitrid bazlı alternatifler değerlendirilmiş, malzemelerin kimyasal ve fiziksel stabilitesi, erime, kaynama ve buna bağlı operasyon sıcaklıkları verilmiş ve alternatifler buna bağlı olarak değerlendirilmiştir.

Hızlandırıcılar için ana iki ayırım olan siklotron ve çizgisel hızlandırıcılar değerlendirilmiştir.



Soğutucular için ise kurşun-kurşun bismut, tuz ve gaz seçenekleri değerlendirilmiş ve ısı iletim özellikleri, faz değiştirme sıcaklıkları ve diğer parametreleri uygunluklarına göre ifade edilmiştir.

Hedef için de, kabul görmüş en uygun alternatif kurşun ile ilgili bilgi verilmiş ve operasyon kapsamında gerekli bilgiler ifade edilmiştir

Takiple kaynak tahrikli alt kritik sistemler tasarımı için kritik olan çoğaltma katsayısı, alt kritik çoğaltma katyayısı ve kaynak verimliliği kavramlarının teorik arka planı aktarılmış ve açıklanmıştır. Kaynak verimliliğinin analitik şekilde elde edilmesi, geride takip eden çoğaltma katsayısı ve alt kritik çoğaltma katyayısı kavramlarına ciddi şekilde bağlıdır. Bu yüzden tezin takip eden her analitik çözüm içeriğinde bu parametreler de hesaplanmış ve sunulmuştur.

Dört adet küresel koordinatta analitik çözümü elde edilmiş problem değerlendirilmiştir:

“Tek grup tek bölge sabit kaynak”, tek enerji gruplu tek boyutlu sistemin tümünde bulunan bir kaynak için alt kritik sistemin analitik olarak çoğaltma katsayısı ve alt kritik çoğaltma katyayısı ve kaynak verimliliği çözümlerini vermektedir.

“Tek Grup Tek Bölge lokalize kaynak”, tek enerji gruplu tek boyutlu bir sistemde lokalize bir kaynağın sistem içerisinde herhangi bir konumu için alt kritik sistemin analitik olarak çoğaltma katsayısı ve alt kritik çoğaltma katyayısı ve kaynak verimliliği çözümlerini vermektedir.

“Birinci bölgede sabit kaynak olmak üzere tek grup iki bölge”, tek enerji gruplu tek boyutlu ancak iki bölgeden, bir tanesi kaynak yarıçapı ve bir tanesi yakıt bölgesi olmak üzere, oluşan alt kritik sistemin değişen kaynak yarıçapına ve sistem yarıçapına göre analitik olarak çoğaltma katsayısı ve alt kritik çoğaltma katyayısı ve kaynak verimliliği çözümlerini vermektedir

“İki Grup Tek Bölge nokta kaynak”. İki enerji gruplu tek boyutlu bir sistemde noktasal bir kaynağın sistem içerisinde herhangi bir konumu için alt kritik sistemin analitik olarak kaynak çarpan, alt kritik çarpan ve kaynak verimliliği çözümlerini vermektedir.

Bu dört incelemeyi takiple, elde edilme denklem setleri MATHEMATICA yardımı ile modellenmiş, sistem boyutu, kaynak konumu veya boyutuna göre çoğaltma katsayısı ve alt kritik çoğaltma katyayısı ve kaynak verimliliğinin değişimleri gözlemlenmiş, elde edilen sonuçlar, beklenen sonuçlar ile karşılaştırmalı olarak incelenmiştir. Buna bağlı yorumlar ifade edilmiştir.

Elde edilen analitik çözümlerin doğruluğunun teyidi için, çok gruplu sonlu fark difüzyon kodu DIFSP yardımı ile, analitik sonuçlar ve numerik çözümler karşılaştırılmıştır. Gerek Mathematica’da gerekse difüzyon kodunda kullanılan tüm nükleer parametreler verilmiş ve ortaya çıkan kaynak çarpan, alt kritik çarpan ve kaynak verimliliğinin karşılaştırmaları yapılmış ve hata oranları paylaşılmıştır. Hakeza difüzyon kodunda ızgara için kullanılan nokta sayıları ve varsa lokalize kaynağın bulunduğu noktalar ifade edilmiştir.

Analitik çözümlerin doğruluğu teyit edildikten sonra, kaynak verimliliği konsepti kaynak tahrikli alt kritik sistemlere dair parametrelerle karşılaştırmalı şekilde incelenmiştir.

Hedef bölgesi boyutları ile kaynak verimliliği ilişkisi incelenmiş, sonuçları tablo ve grafikler yardımı ile ayrıntılı olarak paylaşılmış ve çıktılar tartışılmıştır.

Yakıt bölgesi boyutları ve kaynak verimliliği ilişkisi incelenmiş sonuçları grafik olarak paylaşılmış ve çıktılar tartışılmıştır.

İlgili hesaplardan ve incelemelerden sonra, kaynak tahrikli alt kritik sistem için bir yakıt alternatifi olarak amerisyum ve plutonyum karışımı önerilmiştir. İlgili

malzemeler için fisyon tesir kesitleri ve diđer nükleer sabitler sunulmuş, yakıt için temel parametreler örnek olarak hesaplanmıştır.

Daha sonra, ilgili karışımın deđişen malzeme yüzdelerine göre yakıtın davranışı incelenmiş ve temel parametre ve sonuçlar tablo olarak sunulmuştur. Yine grafiklerle bu deđişim ifade edilmiş ve çıktıları tartışılmıştır.

Son olarak, tüm sonuçların kısa bir özeti ve buradan yapılan çıkarım sunulmuştur.

## 1. INTRODUCTION

Accelerator Driven Systems (ADS) are fission reactors, which are designed especially for the safe burnup of minor actinides, which constitute an important part of high level nuclear waste produced during the operation of nuclear power reactors.

Assuming that the uranium and the plutonium have been separated, high level nuclear waste consists of fission products and minor actinides. The majority of fission products have short enough half-lives so that they decay almost totally in a few centuries. Hence the fission products do not constitute a waste problem in the long run. On the other hand, minor actinides, namely neptunium, americium and curium, continue to contribute strongly to the radiotoxicity of the nuclear waste during the whole first millennium. If minor actinides are separated (partitioned) from the spent fuel and then transformed to nuclei with short half-lives (transmuted), it would be a major step towards the solution of high level nuclear waste problem. This process is called partitioning and transmutation (P&T) and is the subject of active research and development in almost all developed countries involved in nuclear power production. Minor actinides can be transmuted by fissioning to fission products in classical nuclear reactors, which are critical systems. They can also be transmuted by fissioning into fission products in subcritical nuclear systems in which steady-state operation can only be maintained through the introduction of external neutron sources. Such systems are called source-driven subcritical reactors. If the external neutron source is supplied by operating a charged particle accelerator (a proton accelerator in practice), the source-driven subcritical reactor is called an accelerator driven system or ADS (Ozgener, 2009).

Certain safety issues arise when minor actinides are introduced into the nuclear fuel in critical nuclear reactors. These issues stem from the degradation of certain reactivity coefficients when minor actinide containing fuels are used. The use of

source-driven subcritical systems is proposed to overcome these safety issues (Carlo Rubbia, 1996).

Critical nuclear reactors are of two types: thermal reactors and fast reactors. In thermal reactors with low enriched (U, Pu) O<sub>2</sub> fuel, the Doppler broadening of the resonances with increasing fuel temperature creates negative reactivity feedback and constitutes the major inherent safety also in fast reactors. Doppler broadening provides less negative feedback in fast reactors since neutrons are less affected from the major resonances, which lie at lower energies. Minor actinides can also be most efficiently incinerated in fast systems since an important part of the neutron energy spectrum is above the fission threshold of minor actinides. When minor actinides are introduced into the fast reactor fuel, the negative Doppler feedback is lost to a great extent and safety problems may ensue in fast critical systems (Marcus Eriksson, 2005). Thus, the incineration of minor actinides in fast but subcritical systems turns out to be a viable alternative. But subcritical systems need external neutron sources to render steady-state operation possible. By the bombardment of certain nuclei like lead by accelerated proton beams, it is possible to cause neutron producing spallation reactions in the target. These spallation neutrons constitute an adequate external neutron source for subcritical systems. Thus accelerator driven fast subcritical nuclear reactors seem to be a good choice for incinerating minor actinides without causing any safety problems. In most accelerators driven reactor designs liquid lead is proposed also as the coolant. But liquid lead results in a positive void coefficient in a fast neutron spectrum. Thus there is a definite need for sub criticality in fast systems used for incineration of minor actinides.

The criticality level of sourceless nuclear systems is expressed most conveniently by the effective multiplication factor,  $k_{eff}$ . It turns out that the criticality level of subcritical systems which maintain steady-state operation with the aid of an external neutron source is more adequately expressed by a different quantity, namely the subcritical multiplication factor,  $k_s$  (Kobayashi, K., and Nishihara, K., 2000).

In Chapter 2, the major components of accelerator driven systems will be briefly reviewed. We will introduce and the concepts of the subcritical multiplication factor, source multiplication and neutron source efficiency in Chapter 3. Chapter 4 involves the derivation of analytical solutions for neutron flux and  $k_s$  for subcritical system models with localized and extended external sources in one and two group neutron

diffusion theories. For model problems spherically symmetric systems will be utilized. The variation of the subcritical multiplication factor, source multiplication and neutron source efficiency with respect to source location and system dimensions will be studied with the objective of determining the conditions leading to maximum source efficiency. Chapter 5 is about the utilization of the multigroup diffusion finite difference program DIFSP (Ozgener, 2012) for the solution of more realistic model problems for which analytical solutions do not exist. The variation of the source efficiency with respect to target and blanket dimensions will be investigated. The dependence of the source efficiency on the americium to plutonium ratio in the ADS blanket will be studied. The thesis commences with Chapter VI which contains the conclusions and recommendations for further study.



## 2. A BRIEF REVIEW OF THE BASICS OF ACCELERATOR DRIVEN SYSTEMS

### 2.1 Transmutation of Actinides for Solution of the Nuclear Waste Problem

Most of the fuel material discharged from a nuclear reactor still consists of the original uranium (95%), while about 4% has been converted to fission products and about 1% to transuranic elements (Seltborg, 2005). As seen in Figure 1 radiotoxic inventory stemming from fission products is reduced to the level of natural uranium in a few hundred years. In later times, the radiotoxic inventory is almost wholly dominated by the transuranic. If plutonium is separated by reprocessing and reutilized as fuel in nuclear reactors, the major source of radiotoxicity is the minor actinides. Thus, partitioning and transmutation of the minor actinides is one of the major challenges to be met if the solution of the nuclear waste problem is to be found and the sustainability of the nuclear power is to be proved.

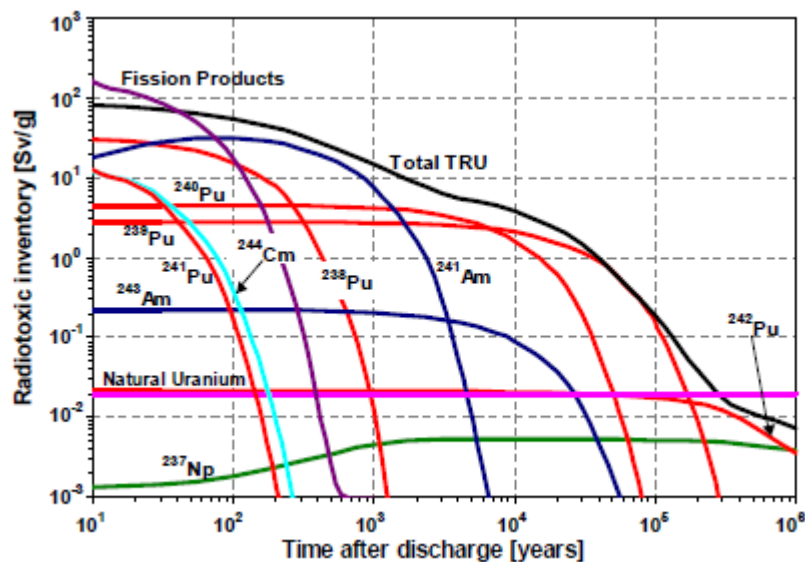


**Figure 2.1 :** Variation of Radiotoxic Inventory Respect to Time in Discharged Fuel.

The domination of radiotoxicity by the actinides stems from their long half-lives compared to the fission products. A review of Figure 2 reveals this fact.

Actinides				Half-life	Fission products
<sup>244</sup> Cm	<sup>241</sup> Pu f	<sup>250</sup> Cf	<sup>243</sup> Cm f	10–30 y	<sup>137</sup> Cs <sup>90</sup> Sr <sup>85</sup> Kr
<sup>232</sup> U f		<sup>238</sup> Pu	f is for	69–90 y	<sup>151</sup> Sm nc→
4n	<sup>245</sup> Cf f	<sup>242</sup> Am f	fissile	141–351	No fission product has half-life 10 <sup>2</sup> to 2×10 <sup>5</sup> years
	<sup>241</sup> Am		<sup>251</sup> Cf f	431–898	
<sup>240</sup> Pu	<sup>229</sup> Th	<sup>246</sup> Cm	<sup>243</sup> Am	5–7 ky	
	<sup>245</sup> Cm f	<sup>250</sup> Cm	<sup>239</sup> Pu f	8–24 ky	
4n	<sup>233</sup> U f	<sup>230</sup> Th	<sup>231</sup> Pa	32–160	
	<sup>234</sup> U			211–290	<sup>99</sup> Tc <sup>126</sup> Sn <sup>79</sup> Se
<sup>248</sup> Cm	4n+1	<sup>242</sup> Pu	4n+3	340–373	Long-lived fission products
	<sup>237</sup> Np			1–2 my	<sup>87</sup> Zr <sup>135</sup> Cs nc→
<sup>238</sup> U		4n+2	<sup>247</sup> Cm f	6–23	<sup>107</sup> Pd <sup>129</sup> I
<sup>244</sup> Pu	4n+1			80 my	>7% >5% >1% >.1%
<sup>232</sup> Th		<sup>238</sup> U	<sup>235</sup> U f	0.7–12by	fission product yield

**Figure 2.2 :** Half-lives of Actinides and Fission Products.

Majority of these major (plutonium and uranium isotopes) and minor (americium, curium, neptunium isotopes) actinides can fissioned and transmuted into fission products in a fast reactor environment. This means minor actinides can be incinerated and at the same time the fission energy can be unleashed.

## 2.2 Components of Accelerator Driven Systems

A typical ADS, as depicted in figure 3, consists of Proton accelerator, Spallation target, Fuel elements, Coolant.

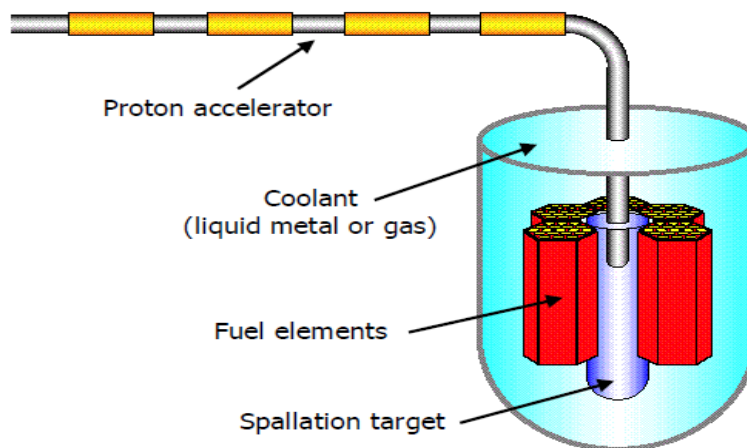


**Figure 2.3 :** Components of an ADS.

### 2.2.1 Proton accelerator

Proton accelerator can be of two types, linear accelerator or cyclotron accelerator



### **2.2.1.1 Linear accelerators**

The basic principle of a linear accelerator, commonly called LINAC, is that the charged particles are accelerated, either by electrostatic fields or oscillating radio-frequency (RF) fields, along a straight line. The particles travel through a series of hollow “drift tubes”, alternately connected to the opposite poles of an AC voltage source. The energy transfer to the particles occurs in the electric field between the tubes, whereas the inside of the tubes are field-free (hence the name, “drift tube”). The polarity of the voltage is reversed while the particles are travelling inside the tubes and the lengths of the tubes are chosen so that the particles reach the gap between the tubes at the moment when the electric field is accelerating. As the velocity of the particles increases, the length of the tubes must also increase, approaching a constant value as the particles become relativistic. In order to reach high energies, since the final energy of the particles is equal to the sum of the voltages to which they have been exposed, either the number of tube segments or the voltage of the RF-source may be increased. As the velocity of the particles quickly becomes high, it is desirable that the RF-frequency is high in order to keep the tube lengths reasonably short (Per Seltborg, 2005).

### **2.2.1.2 Cyclotron accelerators**

A cyclotron is a circular accelerator consisting of two large dipole magnets and two semi-circular metal chambers, called “dees” because of their shape, in which the particles orbit the dees, which are connected to an oscillating voltage, generating an alternating electric field in the gap between the two dees. When they are inside the dees, however, they sense no electric field and follow a circular path until they reach the gap and are accelerated again. In this way, the particles that are emitted at the center of the device follow a spiral path, gaining a certain amount of energy each cycle, until they become energetic enough to leave the accelerator (Per Seltborg, 2005).

### **2.2.2 Spallation target**

Nuclear spallation is one of the processes by which a particle accelerator may be used to produce a beam of neutrons. Mercury, tantalum, lead or other heavy metal, liquid or solid, target can be used, and 20 to 30 neutrons are expelled after each impact. Although this is a far more expensive way of producing neutron beams than

by a chain reaction of nuclear fission in a nuclear reactor, it has the advantage that the beam can be pulsed with relative ease. The main advantages of liquid metals are the superior heat removal capabilities and the significant reduction of the radiation damage to the target (Paul Scherrer Institut, 2006).

Traditional spallation target at the time for ADS is solid lead. Among the studied heavy liquid metals however LBE (Lead Bismuth eutectic) have emerged as a primary candidate. LBE has the clear advantage of having a low melting temperature (123.5 °C) and a boiling temperature of 1,670 °C, which would simplify the heating of the system before operation, as well as reducing the risk of target solidification in case of beam interruption or reactor shutdown. If LBE is chosen as core coolant material, full compatibility between the target loop and the core coolant primary loop could also be achieved (Handbook on Lead-bismuth Eutectic Alloy and Lead Properties, 2007).

### **2.2.3 Fuel elements**

Fuel element options for ADS, which consists of minor actinides, plutonium, and if possible no uranium, need to be irradiated to high burn up to reach high levels of transmutation. This naturally implies that this area is still subject to investigation since while there is extensive knowledge of uranium based fuels, there is little knowledge of minor actinides and plutonium based fuels. Several different options of advanced fuels are being investigated; oxides, nitrides and possibly metal fuels being the most promising (R. J. M. Konings, 2001).

#### **2.2.3.1 Oxide fuels**

With respect to other fuel choices, MOX fuel operation and fabrication is thoroughly investigated by industry. Still, since this knowledge is derived from studies of uranium based fuels, there are many aspects that need further study for the assessment of minor actinides containing oxide fuels (R. J. M. Konings, 2001). Among the negative consequences of going from a uranium-based fuel to fuels containing high fractions of plutonium and MA are lower melting point (decreases with increasing atomic number, from  $\text{UO}_2$  (3113 K) to  $\text{AmO}_2$  (2448 K)), lower thermal conductivity and poorer chemical stability. Moreover, a general problem for all fuel forms with high MA content is the helium gas production, leading to

intolerable swelling of the fuel. Another major drawback of oxide fuels is the low thermal conductivity, leading to high operating temperatures (Per Seltborg, 2005).

Even with respect to these drawbacks however, oxide fuels have high chemical stability, which makes both fabrication and safety requirements simpler

### **2.2.3.2 Nitride fuels**

Nitride fuels have five times higher thermal conductivity than uranium based oxide fuels but similar melting temperatures. Thus, lower operating temperatures are possible for nitride fuels. Various actinide nitrides show good mutual miscibility and it is therefore expected that the solid solution (Np, Pu, Am, Cm) can exist over a wide range of compositions. Actinide nitrides are also compatible with the PUREX method. It also possesses chemical compatibility with water, air and stainless steel cladding materials (Per Seltborg, 2005).

Nitride fuels are poor in terms of chemical and thermal stability, which proves to be a problem in terms of safety and fabrication.

Further, the addition of an inert matrix, ZrN for example, is expected to improve the thermal stability of nitride fuels. Another disadvantage of nitride fuels is the production of  $^{14}\text{C}$  from  $^{14}\text{N}$ . This may require the enrichment of  $^{15}\text{N}$  (J. Wallenius and S. Pillon, 2001).

### **2.2.3.3 Metal fuels**

Metallic fuels have high thermal conductivity and high melting temperature (1620 K) for uranium based alloys. However, with the addition of plutonium and minor actinides, these favorable properties drop drastically and hence the addition of an inert matrix is required, of which the most promising candidate is zirconium with a melting point of 2128 K. Another disadvantage of metallic fuels is their incompatibility with LBE (Per Seltborg, 2005).

### **2.2.4 Coolant**

Since ADS by the nature of its design is a fast reactor, the first element to be recognized is, water as a coolant will not serve this purpose due to its highly moderating properties. Hence, with respect to fast neutron spectrum, the preferences are reduced to liquid metals and gas. But to cool the core with a gas coolant, high

pressure must be applied. However on the contrary to gas option, liquid metal has positive void worth and opacity (J. Wallenius, 2003).

#### 2.2.4.1 Lead or lead-bismuth eutectic

Since lead or lead bismuth eutectic can be same as spallation target, the necessity for separation of spallation target and reactor can be avoided. Lead bismuth has a boiling temperature of 1670 °C, which is an advantage for the core cooling problems hence an accident due to coolant loss is unlikely. Also, while lead melts at 327.5 °C, which derives problems at refueling and shutdown due to solidification of coolant and high operating temperatures (400-600 °C) that cause corrosion, with lead-bismuth  $T_{melt}$  is only 123.5 °C and therefore has a relatively low operating temperature of 200 °C (Handbook on Lead-bismuth Eutectic Alloy and Lead Properties, 2007).

Bismuth as a coolant (or spallation target) on the other hand, produces  $^{210}\text{Po}$ , which emits alpha particles and has a half-life of 138 days. Therefore a confinement for coolant must be administered for Lead-Bismuth Eutectic.

**Table 2.1** : Physical properties of the main liquid metal coolant options (Per Seltborg, 2005).

<b>Material</b>	<b><math>\sigma</math>[g/cm<sup>3</sup>] (~400 °C)</b>	<b><math>T_{melt}</math> [°C]</b>	<b><math>T_{boil}</math> [°C]</b>	<b><math>k</math> [W/m K]</b>	<b><math>C_p</math> [J/kg K]</b>
<b>Pb</b>	11.07	327.5	1749	16	150
<b>LBE</b>	10.24	123.5	1670	12.9	147
<b>Na</b>	0.857	97.7	883	71.6	1300

#### 2.2.4.2 Sodium

Sodium has been used for fast critical reactors and therefore there is extensive knowledge about its operational properties. Since Sodium has very good thermal property such as high thermal conductivity, it is a reliable coolant and a core cooling problem is unlikely. However a high positive void worth and reactivity with air and water are constant problems for the sodium coolants (J. Wallenius, 2003).

#### 2.2.4.3 Gas

With the gas option (He or CO<sub>2</sub>), it is possible to get a hard neutron energy spectrum and gas has almost zero positive void worth, since gases are transparent to neutrons.

In the case of helium, it is a noble gas and does not interact therefore chemical setbacks with structural materials are eluded easily. However, to serve as a coolant, gas needs to be pressurized at a value of 50-70 bars. This would put heat removal at risk in an emergency scenario since it is easy to lose coolant and bring a necessity to physically separate coolant from reactor core (Per Seltborg, 2005).



### 3. SOURCE MULTIPLICATION , SUBCRITICAL MULTIPLICATION FACTOR AND SOURCE EFFICIENCY

#### 3.1 Neutron Importance Function

The multigroup diffusion equations for a subcritical, source-driven system at steady state can be expressed in matricial form as:

$$L\phi = \chi\vartheta\Sigma_f^T\phi + s \quad (3.1)$$

Where

$$L = \begin{bmatrix} -\vec{\nabla}D_I\vec{\nabla} + \Sigma_{rI} & 0 & \dots & 0 \\ -\Sigma_{s21} & -\vec{\nabla}D_{II}\vec{\nabla} + \Sigma_{rII} & 0 & 0 \\ \dots & \dots & \dots & \dots \\ -\Sigma_{sG1} & -\Sigma_{sG2} & -\Sigma_{sG3} & -\vec{\nabla}D_G\vec{\nabla} + \Sigma_{aG} \end{bmatrix} \quad (3.2)$$

$$\phi^T = [\phi_I\phi_{II} \dots \phi_G] \quad (3.3)$$

$$\chi = [\chi_I\chi_{II} \dots \chi_G] \quad (3.4)$$

$$\vartheta\Sigma_f^T = [\vartheta\Sigma_{fI}\vartheta\Sigma_{fII} \dots \vartheta\Sigma_{fG}] \quad (3.5)$$

$$s^T = [s_I s_{II} \dots s_G] \quad (3.6)$$

where G is the number of groups.

On the other hand, an adjoint problem can be defined as (Jeffery Lewins, 1965)

$$L^T\phi^+ = \vartheta\Sigma_f\chi^T\phi^+ + \vartheta\Sigma_f \quad (3.7)$$

Premultiplying Eq. (3.1) by  $\phi^{+T}$  and integrating over the system volume, we obtain:

$$\langle\phi^{+T}L\phi\rangle = \langle\phi^{+T}\chi\vartheta\Sigma_f^T\phi\rangle + \langle\phi^{+T}s\rangle \quad (3.8)$$

where  $\langle\dots\rangle$  denotes integration over the system volume.

Similarly premultiplying Eq.(3.7) by  $\phi^T$  and again intrgrating over the system volume:

$$\langle\phi^TL^T\phi^+\rangle = \langle\phi^T\vartheta\Sigma_f\chi^T\phi^+\rangle + \langle\phi^T\vartheta\Sigma_f\rangle \quad (3.9)$$

Since  $L^T$  is the adjoint operator of  $L$  and  $\vartheta\Sigma_f\chi^T$  is the adjoint operator of  $\chi\vartheta\Sigma_f^T$  (Duderstadt and Hamilton, 1976):

$$\langle\phi^{+T}L\phi\rangle = \langle\phi^TL^T\phi^+\rangle \quad (3.10)$$

$$\langle \phi^{+T} \chi \vartheta \Sigma_f^T \phi \rangle = \langle \phi^T \vartheta \Sigma_f \chi^T \phi^+ \rangle \quad (3.11)$$

Subtracting (3.9) from (3.8) and employing (3.10) and (3.11):

$$\langle \phi^{+T} s \rangle = \langle \phi^T \vartheta \Sigma_f \rangle \quad (3.12)$$

Since  $\phi^T \vartheta \Sigma_f$  is a scalar quantity:

$$\langle \vartheta \Sigma_f^T \phi \rangle = \langle \phi^{+T} s \rangle \quad (3.13)$$

That is, the fission neutron production rate,  $\langle \vartheta \Sigma_f^T \phi \rangle$  can be calculated for any external source vector provided we know  $\phi^+$ . Thus if we solve the adjoint problem (3.7) once, we can determine the fission neutron production rate caused by any external source by (3.13) without solving (1) for  $\phi$ .

To understand the physical meaning of  $\phi^+$ , consider a system in which the only external source is placed is a unit point source at  $\vec{\rho}$  emitting only group-h neutrons. Then only the h th element of  $s$  would be nonzero and that element would be a Dirac delta function. That is:

$$s_g = \delta(\vec{r} - \vec{\rho}) \delta_{gh} \quad (3.14)$$

where  $\delta_{gh}$  is the Kroenecker delta. If we place (3.14) on the right hand side of (3.13) and use the integration property of the Dirac delta function we obtain:

$$\langle \vartheta \Sigma_f^T \phi \rangle = \phi_h^+(\vec{\rho}) \quad (3.15)$$

That is  $\phi_h^+(\vec{\rho})$  is equal to the fission neutron emission rate caused by an external neutron source placed at the point  $\vec{\rho}$  emitting one group h neutron per unit time. If  $\phi_h^+(\vec{\rho})$  is large, then the fission neutron emission rate is also large. That is,  $\phi_h^+(\vec{\rho})$  is a measure of the importance of point  $\vec{\rho}$  and group h in producing fission neutrons in the system. Thus  $\phi_g^+(\vec{r})$  is called the group g neutron importance function and is dimensionless.

### 3.2 Source Multiplication and Reactor Power

Source multiplication,  $M_s$ , is defined as:

$$M_s = \frac{\langle \vartheta \Sigma_f^T \phi \rangle}{\langle u^T s \rangle} \quad (3.16)$$

Here  $u$  is a G dimensional column matrix whose all elements equal one.



Thus  $M_s$  is equal to the ratio of fission neutron emission rate to the external neutron source emission rate. Thus it may be interpreted as the number of fission neutrons emitted per source neutron introduced. In another way, source multiplication characterizes the fission causing capacity of the external neutron source introduced. Using (3.13) in (3.16), we can also write:

$$M_s = \frac{\langle \phi^{+T} S \rangle}{\langle u^T S \rangle} \quad (3.17)$$

From (3.17) it is obvious that the source multiplication,  $M_s$ , is simply a measure of the importance of the external source placed into the system in causing fission.

Consider an accelerator-driven subcritical reactor and let

$P_{beam}$ : The beam power (power required by the proton accelerator)

$\varepsilon_n$ : Energy consumed for production of a source (spallation) neutron

Thus,  $P_{beam}/\varepsilon_n$  gives simply the number of source neutrons produced per unit time.

Thus:

$$\langle u^T S \rangle = \frac{P_{beam}}{\varepsilon_n} \quad (3.18)$$

If we use (3.18) in (3.16) and rearrange, we obtain:

$$\langle \vartheta \Sigma_f^T \phi \rangle = M_s \frac{P_{beam}}{\varepsilon_n} \quad (3.19)$$

Now let

$\vartheta$ : The average number of neutrons emitted per fission in the reactor

$\varepsilon_f$ : Energy released per fission

$P$ : The reactor (thermal) power

then:

$$P = \frac{\varepsilon_f M_s}{\varepsilon_n \vartheta} P_{beam} \quad (3.20)$$

To get the maximum reactor power per unit beam power,  $M_s$  or the source multiplication must be obviously maximized. Since the placement and energy of the external source determines  $M_s$ , the source selection becomes an optimization problem. In this work, we will try to determine the selection of source parameters so that the source multiplication is reasonably well maximized.

### 3.3 Subcritical Multiplication Factor

Many authors in the literature prefer to characterize subcritical, source-driven systems by  $k_s$ , the subcritical multiplication factor.  $k_s$  is defined verbally in analogy to the  $k_{eff}$  of sourceless systems as:

$$k_s = \frac{\text{Fission Neutron Production Rate}}{\text{Neutron Loss (absorption+leakage rate)}} \quad (3.21)$$

Since the neutron loss rate must be equal to the neutron production rate for steady state operation, we can also write:

$$k_s = \frac{\text{Fission Neutron Production Rate}}{\text{Fission Neutron Production Rate} + \text{External Source Neutron Production Rate}} \quad (3.22)$$

Mathematically this could be stated as:

$$k_s = \frac{\langle \vartheta \Sigma_f^T \phi \rangle}{\langle \vartheta \Sigma_f^T \phi \rangle + \langle u^T S \rangle} \quad (3.23)$$

Dividing both the numerator and the denominator of (3.23) by  $\langle u^T S \rangle$  and using the definition of source multiplication in (3.16), it readily follows:

$$k_s = \frac{M_s}{M_s + 1} \quad (3.24)$$

If we solve (3.24) for  $M_s$ , we obtain:

$$M_s = \frac{k_s}{1 - k_s} \quad (3.25)$$

Since  $0 \leq k_s < 1$ , we have  $0 \leq M_s < \infty$  and the maximization of  $M_s$  is equivalent to the maximization of  $k_s$ .

Using (3.25) in (3.20) we can also write:

$$P = \frac{\varepsilon_f}{\vartheta \varepsilon_n} \frac{k_s}{1 - k_s} P_{beam} \quad (3.26)$$

### 3.4 Source Efficiency

Some researchers prefer to use the concept of source efficiency,  $\varphi^*$  instead of source multiplication,  $M_s$ . To understand the concept of source efficiency, we must consider the  $k_{eff}$  problem of the sourceless system (the criticality problem)

$$L\phi_c = \frac{1}{k_{eff}} \chi \vartheta \Sigma_f^T \phi_c \quad (3.27)$$

and the adjoint criticality problem

$$L^T \phi_c^+ = \frac{1}{k_{eff}} \vartheta \Sigma_f \chi^T \phi_c^+ \quad (3.28)$$

$\phi_c^+$  is interpreted as the neutron importance function of the sourceless system (Bell and Glasstone, 1970)

Premultiplying (3.28) by  $\phi_c^T$  and integrating over the system volume,

$$\langle \phi_c^T L \phi_c^+ \rangle = \frac{1}{k_{eff}} \langle \phi_c^T \vartheta \Sigma_f \chi^T \phi_c^+ \rangle \quad (3.29)$$

which yields:

$$\frac{1}{k_{eff}} = \frac{\langle \phi_c^T L \phi_c^+ \rangle}{\langle \phi_c^T \vartheta \Sigma_f \chi^T \phi_c^+ \rangle} \quad (3.30)$$

which can also be written as:

$$\frac{1}{k_{eff}} = \frac{\langle \phi_c^{+T} L \phi \rangle}{\langle \phi_c^{+T} \chi \vartheta \Sigma_f^T \phi \rangle} \quad (3.31)$$

Premultiplying (3.1) by  $\phi_c^{+T}$  and integrating,

$$\langle \phi_c^{+T} L \phi \rangle = \langle \phi_c^{+T} \chi \vartheta \Sigma_f^T \phi \rangle + \langle \phi_c^{+T} S \rangle \quad (3.32)$$

which can be rearranged as

$$\frac{\langle \phi_c^{+T} L \phi \rangle}{\langle \phi_c^{+T} \chi \vartheta \Sigma_f^T \phi \rangle} = 1 + \frac{\langle \phi_c^{+T} S \rangle}{\langle \phi_c^{+T} \chi \vartheta \Sigma_f^T \phi \rangle} \quad (3.33)$$

Using (3.31) in (3.33),

$$\frac{1}{k_{eff}} = 1 + \frac{\langle \phi_c^{+T} S \rangle}{\langle \phi_c^{+T} \chi \vartheta \Sigma_f^T \phi \rangle} \quad (3.34)$$

Multiplying and dividing the numerator of the second term by  $\langle u^T S \rangle$  and multiplying and dividing the denominator of the same term by  $\langle \vartheta \Sigma_f^T \phi \rangle$

$$\frac{1}{k_{eff}} = 1 + \frac{\frac{\langle \phi_c^{+T} S \rangle}{\langle u^T S \rangle}}{\frac{\langle \phi_c^{+T} \chi \vartheta \Sigma_f^T \phi \rangle}{\langle \vartheta \Sigma_f^T \phi \rangle}} \frac{\langle u^T S \rangle}{\langle \vartheta \Sigma_f^T \phi \rangle} \quad (3.35)$$

By (3.16), (3.35) becomes

$$\frac{1}{k_{eff}} = 1 + \frac{\frac{\langle \phi_c^{+T} s \rangle}{\langle u^T S \rangle}}{\frac{\langle \phi_c^{+T} \chi \vartheta \Sigma_f^T \phi \rangle}{\langle \vartheta \Sigma_f^T \phi \rangle}} \frac{1}{M_s} \quad (3.36)$$

By (3.25), (3.36) becomes

$$\frac{1-k_{eff}}{k_{eff}} = \frac{\frac{\langle \phi_c^{+T} s \rangle}{\langle u^T S \rangle}}{\frac{\langle \phi_c^{+T} \chi \vartheta \Sigma_f^T \phi \rangle}{\langle \vartheta \Sigma_f^T \phi \rangle}} \frac{1-k_s}{k_s} \quad (3.37)$$

The first term on the right hand side is defined as the source efficiency,  $\varphi^*$

$$\varphi^* = \frac{\frac{\langle \phi_c^{+T} s \rangle}{\langle u^T S \rangle}}{\frac{\langle \phi_c^{+T} \chi \vartheta \Sigma_f^T \phi \rangle}{\langle \vartheta \Sigma_f^T \phi \rangle}} \quad (3.38)$$

With this definition, the source efficiency is the ratio of average importance of source neutrons to the average importance of fission neutrons. Now we can write:

$$\varphi^* = \frac{\frac{1-k_{eff}}{k_{eff}}}{\frac{1-k_s}{k_s}} \quad (3.39)$$

By (3.39) maximizing  $k_s$  is also equivalent to maximizing the source efficiency.

Combining (3.26) and (3.39):

$$P = \frac{\varepsilon_f}{\vartheta \varepsilon_n} \frac{k_{eff}}{1-k_{eff}} \varphi^* P_{beam} \quad (3.40)$$

## 4. BENCHMARK ANALYTICAL SOLUTIONS

To provide exact results for the assessment of the dependence of source multiplication and related quantities on design parameters, four cases of analytical solutions will be provided in spherical coordinates. Spherical geometry is chosen since it is the only physically realizable one dimensional geometry and is more amenable to analytical solutions.

### 4.1 One Group One Region Flat Source

Since the governing differential equation:

$$-D \frac{1}{r^2} \frac{d}{dr} \left[ r^2 \frac{d\phi_g(r)}{dr} \right] + \Sigma_a \phi_g(r) - \vartheta \Sigma_f \phi_g(r) = q_0 \quad (4.1)$$

is inhomogeneous, the general solution can be written as the sum of homogenous solution and a particular solution.

$$\phi_g(r) = \phi(r) + \phi_p \quad (4.2)$$

An analytical approach for a nuclear system is as follows

First homogenous solution for the equation has to be obtained and therefore equating  $q_0=0$

$$-D \frac{1}{r^2} \frac{d}{dr} \left[ r^2 \frac{d\phi(r)}{dr} \right] + \Sigma_a \phi(r) - \vartheta \Sigma_f \phi(r) = 0 \quad (4.3)$$

For function  $\phi(r)$  a proposition is made

$$\phi(r) = \frac{w(r)}{r} \quad (4.4)$$

We apply the proposition

$$-D \frac{1}{r^2} \frac{d}{dr} r^2 \frac{d}{dr} \frac{w(r)}{r} + \Sigma_a \frac{w(r)}{r} - \vartheta \Sigma_f \frac{w(r)}{r} = 0 \quad (4.5)$$

First derivative for the left hand first term

$$-D \frac{1}{r^2} \frac{d}{dr} r^2 [-r^{-2} w(r) + w(r)' r^{-1}] + \Sigma_a \frac{w(r)}{r} - \vartheta \Sigma_f \frac{w(r)}{r} = 0 \quad (4.6)$$

Second Derivative for the left hand first term

$$-D \frac{1}{r^2} \frac{d}{dr} [-w(r) + w(r)'r] + \sum_a \frac{w(r)}{r} - \vartheta \sum_f \frac{w(r)}{r} = 0 \quad (4.7)$$

$$-D \frac{1}{r^2} [-w(r)' + w(r) + w(r)''r] + \sum_a \frac{w(r)}{r} - \vartheta \sum_f \frac{w(r)}{r} = 0 \quad (4.8)$$

Hence

$$\frac{-D}{r} [w(r)''] + \sum_a \frac{w(r)}{r} - \vartheta \sum_f \frac{w(r)}{r} = 0 \quad (4.9)$$

$$w(r)'' + \left( \frac{\vartheta \sum_f}{D} - \frac{\sum_a}{D} \right) w(r) = 0 \quad (4.10)$$

$$L^2 = \frac{D}{\sum_a} \quad (4.11)$$

$$w(r)'' + \left( \frac{\vartheta \sum_a \sum_f}{\sum_a D} - \frac{\sum_a}{D} \right) w(r) = 0 \quad (4.12)$$

$$w(r)'' + \frac{1}{L^2} \left( \frac{\vartheta \sum_f}{\sum_a} - 1 \right) w(r) = 0 \quad (4.13)$$

$$k_\infty = \frac{\vartheta \sum_f}{\sum_a} \quad (4.14)$$

$$w(r)'' + \frac{1}{L^2} (k_\infty - 1) w(r) = 0 \quad (4.15)$$

Value of  $B_m$  being

$$B_m^2 = \frac{k_\infty - 1}{L^2} \quad (4.16)$$

$$w(r)'' + B_m^2 w(r) = 0 \quad (4.17)$$

This equation is a Helmholtz equation, to which a set of solution may be proposed.

However for the sake of practicality, the transformation will be applied now

$$w(r) = \varnothing(r).r$$

$$w(r)' = \varnothing(r)' . r + \varnothing(r)$$

$$w(r)'' = \varnothing(r)'' . r + 2\varnothing(r)'$$

Applying these values

$$r^2 \varnothing(r)'' + 2r \varnothing(r)' + r^2 B_m^2 \varnothing(r) = 0 \quad (4.18)$$

This is a denigrated form of spherical Bessel equation which is

$$r^2 \frac{d^2 \phi(r)}{dr^2} + 2r \frac{d\phi(r)}{dr} + [r^2 k^2 - l(l+1)]\phi(r) = 0 \quad (4.19)$$

Therefore  $l$  is obtained as  $l=0$ . For an analytical spherical Bessel equation a solution may be proposed that consists of two parts

$$j_l(r) = (-r)^l \left[ \frac{1}{r} \frac{d}{dr} \right]^l \frac{\sin(r)}{r} \quad (4.20)$$

$$y_l(r) = -(-r)^l \left[ \frac{1}{r} \frac{d}{dr} \right]^l \frac{\cos(r)}{r} \quad (4.21)$$

$$\text{Since } l=0 \quad (4.22)$$

$$j_0(r) = \frac{\sin(r)}{r} \quad (4.23)$$

$$y_0(r) = -\frac{\cos(r)}{r} \quad (4.24)$$

By applying boundary conditions an analytical solution can be obtained

$$\text{For } r \rightarrow 0 \quad \phi(r) \neq \infty$$

Therefore the  $y$  part of the solution is cancelled

$$\text{For } r \rightarrow R_0 \quad \phi(r) = 0; k^2 = B_m^2$$

$$\phi(r) = j_0(kr) = A \frac{\sin(kr)}{r}$$

$$A \frac{\sin(B_m R_0)}{R_0} = 0$$

For the sine function to be equal to 0, it must be in the form of an integer multiplied by  $\pi$

$$B_m R_0 = n\pi$$

Taking  $n=1$ , the radius for criticality is obtained

$$R_0 = \frac{\pi}{B_m}$$

Hence the analytical solution for  $\phi(r)$  is

$$\phi(r) = A \frac{\sin(B_m r)}{r} \quad (4.25)$$

For particular solution, since solution is constant the derivative part cancels

$$\phi_p(\Sigma_a - \vartheta\Sigma_f) = q_o \quad (4.26)$$

$$-\phi_p B_m^2 = \frac{q_o}{D}$$

$$\phi_p = -\frac{q_o}{B_m^2 D}$$

Therefore solution

$$\phi_g(r) = A \frac{\sin(B_m r)}{r} - \frac{q_o}{B_m^2 D} \quad (4.27)$$

This equation has to satisfy the boundary condition

$$\text{For } r \rightarrow R_0 \quad \phi(r) = 0$$

Therefore

$$\phi_g(R_0) = A \frac{\sin(B_m R_0)}{R_0} - \frac{q_o}{B_m^2 D} = 0 \quad (4.28)$$

$$A \frac{\sin(B_m R_0)}{R_0} = \frac{q_o}{B_m^2 D} \quad (4.29)$$

$$A = \frac{R_0}{\sin(B_m R_0)} \frac{q_o}{B_m^2 D} \quad (4.30)$$

To obtain the general solution

$$\phi_g(r) = \frac{R_0}{\sin(B_m R_0)} \frac{q_o}{B_m^2 D} \frac{\sin(B_m r)}{r} - \frac{q_o}{B_m^2 D} \quad (4.31)$$

$$\phi_g(r) = \frac{q_o}{B_m^2 D} \left[ \frac{R_0}{r} \frac{\sin(B_m r)}{\sin(B_m R_0)} - 1 \right]$$

To simplify denotations

$$\phi_g(r) = \frac{q_o}{D B_m^2} \left[ \frac{B_m R_0}{B_m r} \frac{\sin(B_m r)}{\sin(B_m R_0)} - 1 \right]$$

$$y = B_m r ; x = B_m R_0 ; D B_m^2 = (k_\infty - 1) \Sigma_a$$

$$\phi_g(x, y) = \left( \frac{x \sin y}{y \sin x} - 1 \right) \frac{q_o}{(k_\infty - 1) \Sigma_a} \quad (4.32)$$

where  $0 < x < \pi$  and  $0 < y < x$

Since the general solution is obtained,  $k_s$  which is the alternative multiplication constant of the system can be obtained



$$k_s = \frac{S}{S + Q}$$

Where S is the total number of fission neutrons and Q is total number of source neutrons.

$$\phi_I = \frac{q_0}{DB_m^2}; \phi_g(r) = \phi_I \varphi(r)$$

$$k_s = \frac{\vartheta \Sigma_f \int_0^{R_0} \phi_g(r) 4\pi r^2 dr}{\left( \vartheta \Sigma_f \int_0^{R_0} \phi_g(r) 4\pi r^2 dr + q_0 \int_0^{R_0} 4\pi r^2 dr \right)} \quad (4.33)$$

$$k_s = \frac{1}{1 + \frac{q_0 \int_0^{R_0} r^2 dr}{\vartheta \phi_I \Sigma_f \int_0^{R_0} r^2 \varphi_g(r) dr}} \quad (4.34)$$

$$k_s = \frac{1}{1 + \frac{q_0 R_0^3}{3 \vartheta \phi_I \Sigma_f \int_0^{R_0} r^2 \varphi_g(r) dr}} \quad (4.35)$$

For the remaining integration

$$\begin{aligned} \int_0^{R_0} r^2 \varphi_g(r) dr &= \int_0^{R_0} r^2 \left[ \frac{R_0 \sin(B_m r)}{r \sin(B_m R_0)} - 1 \right] dr \\ &= \int_0^{R_0} \frac{R_0 r \sin(B_m r)}{\sin(B_m R_0)} dr - \int_0^{R_0} r^2 dr \\ &= \frac{R_0}{\sin(B_m R_0)} \int_0^{R_0} r \sin(B_m r) dr - \frac{R_0^3}{3} \end{aligned}$$

To solve the integration, integration by parts must be applied

$$\int u dv = uv - \int v du$$

$$u = r; dv = \sin(B_m r) dr; du = dr; v = -\frac{\cos(B_m r)}{B_m}$$

$$\begin{aligned} \int_0^{R_0} r \sin(B_m r) dr &= -\frac{R_0 \cos(B_m R_0)}{B_m} + \int_0^{R_0} \frac{\cos(B_m r)}{B_m} dr \\ &= \frac{\sin(B_m R_0)}{B_m^2} - \frac{R_0 \cos(B_m R_0)}{B_m} \end{aligned}$$

Therefore

$$\begin{aligned}
\int_0^{R_0} r^2 \varphi_g(r) dr &= \frac{R_0}{\sin(B_m R_0)} \left[ \frac{\sin(B_m R_0)}{B_m^2} - \frac{R_0 \cos(B_m R_0)}{B_m} \right] - \frac{R_0^3}{3} \\
&= \left[ \frac{R_0 \sin(B_m R_0)}{B_m^2 \sin(B_m R_0)} - \frac{R_0^2 \cos(B_m R_0)}{B_m \sin(B_m R_0)} \right] - \frac{R_0^3}{3} \\
&= \left[ \frac{R_0}{B_m^2} - \frac{R_0^2 \cot(B_m R_0)}{B_m} \right] - \frac{R_0^3}{3} \\
&= \frac{R_0}{B_m^2} \left[ 1 - B_m R_0 \cot(B_m R_0) - \frac{(B_m R_0)^2}{3} \right]
\end{aligned}$$

Therefore  $k_s$

$$k_s = \frac{1}{1 + \frac{q_0 (B_m R_0)^2}{3 \vartheta \phi_I \Sigma_f \left( 1 - B_m R_0 \cot(B_m R_0) - \frac{(B_m R_0)^2}{3} \right)}} \quad (4.36)$$

To simplify,

$$f(B_m R_0) = \frac{(B_m R_0)^2}{1 - B_m R_0 \cot(B_m R_0) - \frac{(B_m R_0)^2}{3}}$$

$$k_s = \frac{1}{1 + \frac{q_0}{3 \vartheta \phi_I \Sigma_f} f(B_m R_0)}$$

$$\phi_I = \frac{q_0}{D B_m^2}$$

$$k_s = \frac{1}{1 + \frac{D B_m^2}{3 \vartheta \Sigma_f} f(B_m R_0)} = \frac{1}{1 + \frac{L^2 B_m^2}{3 k_\infty} f(B_m R_0)}$$

$$B_m^2 = \frac{k_\infty - 1}{L^2}; \quad \frac{L^2 B_m^2}{k_\infty} = \frac{L^2 (k_\infty - 1)}{L^2 k_\infty} = \frac{(k_\infty - 1)}{k_\infty}$$

$$k_s = \frac{1}{1 + \frac{k_\infty - 1}{3 k_\infty} f(B_m R_0)}$$

$$x = B_m R_0$$

$$f(B_m R_0) = f(x) = \frac{x^2}{1 - x \cot(x) - \frac{x^2}{3}}$$

$$k_s = \frac{1}{1 + \frac{(k_\infty - 1)x^2}{k_\infty(3 - 3x \cot(x) - x^2)}}$$

$$k_s = \frac{k_\infty(3 - 3x \cot(x) - x^2)}{k_\infty(3 - 3x \cot(x) - x^2) + (k_\infty - 1)x^2}$$

$$k_s = \frac{3 - 3x \cot(x) - x^2}{3 - 3x \cot(x) - x^2 + \frac{(k_\infty - 1)}{k_\infty}x^2}$$

$$k_s = \frac{-1 + x \cot(x) + x^2/3}{-1 + x \cot(x) + x^2/3k_\infty}$$

$$k_s = \frac{1 - x \cot(x) - x^2/3}{1 - x \cot(x) - x^2/3k_\infty} \quad (4.37)$$

$$k_{eff} = \frac{(B_m R_0)^2 k_\infty}{(B_m R_0)^2 + (k_\infty - 1)\pi^2} \quad (4.38)$$

$$M_s = \frac{k_s}{1 - k_s}$$

$$\varphi^* = \frac{1 - k_{eff}}{k_{eff}} M_s$$

## 4.2 One Group One Region Dirac Source

To obtain a solution for a localized source, the equation must be solved for two multiplying regions that are divided by a Dirac delta source, which will be calculated through boundary condition;

Which

$$-D \frac{1}{r^2} \frac{d}{dr} \left[ r^2 \frac{d\phi(r)}{dr} \right] + \Sigma_a \phi(r) - \vartheta \Sigma_f \phi(r) = \delta(r - r_0) q_0 \quad (4.39)$$

For both the first and second region which are multiplying and without a source

$$-D \frac{1}{r^2} \frac{d}{dr} \left[ r^2 \frac{d\phi(r)}{dr} \right] + \Sigma_a \phi(r) - \vartheta \Sigma_f \phi(r) = 0 \quad (4.40)$$

The solution can be obtained as

$$\phi_I(r) = A \frac{\sin(B_m r)}{r} + B \frac{\cos(B_m r)}{r}$$

$$\phi_{II}(r) = C \frac{\sin(B_m r)}{r} + D \frac{\cos(B_m r)}{r}$$

For  $r \rightarrow 0$   $\phi_I(r) \neq \infty$

Therefore

$$\phi_I(r) = A \frac{\sin(B_m r)}{r} \quad (4.41)$$

For  $r \rightarrow R_0$   $\phi_{II}(r) = 0$

$$\phi_{gII}(R_0) = C \frac{\sin(B_m R_0)}{R_0} + D \frac{\cos(B_m R_0)}{R_0} = 0$$

For that to be possible

$$C \sin(B_m R_0) + D \cos(B_m R_0) = 0$$

$$D = -C \frac{\sin(B_m R_0)}{\cos(B_m R_0)}$$

$$\phi_{II}(r) = \frac{C \sin(B_m r) \cos(B_m R_0) - \sin(B_m R_0) \cos(B_m r)}{r \cos(B_m R_0)} \quad (4.42)$$

$$G = -C / \cos(B_m R_0)$$

$$\phi_{II}(r) = G \frac{\sin(B_m R_0 - B_m r)}{r} \quad (4.43)$$

Two regions have boundary conditions with respect to their intersection point

$$\phi_{gI}(r_0) = \phi_{gII}(r_0)$$

$$-D \frac{d\phi_{gI}(r_0)}{dr} + q_o = -D \frac{d\phi_{gII}(r_0)}{dr}$$

For the first boundary condition

$$G \frac{\sin(B_m R_0 - B_m r_0)}{r_0} = A \frac{\sin(B_m r_0)}{r_0}$$

$$G = A \frac{\sin(B_m r_0)}{\sin(B_m R_0 - B_m r_0)} \quad (4.44)$$

For the second boundary condition

$$\frac{d\phi_{gI}(r)}{dr} = A \left( B_m \frac{\cos(B_m r)}{r} - \frac{\sin(B_m r)}{r^2} \right) = -\frac{A \sin(B_m r)}{r^2} (1 - r B_m \cot(B_m r))$$

$$\frac{d\phi_{gII}(r)}{dr} = G \left( -\frac{\sin(B_m R_0 - B_m r)}{r^2} - \frac{B_m \cos(B_m R_0 - B_m r)}{r} \right)$$

$$\frac{d\phi_{gII}(r)}{dr} = -\frac{G}{r^2} (\sin(B_m R_0 - B_m r) + r B_m \cos(B_m R_0 - B_m r))$$

$$\begin{aligned} \frac{A \sin(B_m r_0)}{r_0^2} (1 - r_0 B_m \cot(B_m r_0)) \\ = \frac{A \sin(B_m r_0) (\sin(B_m R_0 - B_m r_0) + r_0 B_m \cos(B_m R_0 - B_m r_0))}{r_0^2 \sin(B_m R_0 - B_m r_0)} - \frac{q_0}{D} \end{aligned}$$

$$\begin{aligned} A(\sin(B_m r_0) - r_0 B_m \cos(B_m r_0)) \\ = A(\sin(B_m r_0) + r_0 B_m \sin(B_m r_0) \cot(B_m R_0 - B_m r_0)) - \frac{q_0 r_0^2}{D} \end{aligned}$$

$$\begin{aligned} A(\sin(B_m r_0) + r_0 B_m \sin(B_m r_0) \cot(B_m R_0 - B_m r_0)) - \frac{q_0 r_0^2}{D} \\ = \frac{q_0 r_0^2}{D} \end{aligned}$$

$$\begin{aligned} \frac{A r_0 B_m}{\sin(B_m R_0 - B_m r_0)} (\sin(B_m r_0) \cos(B_m R_0 - B_m r_0) \\ + \sin(B_m R_0 - B_m r_0) \cos(B_m r_0)) = \frac{q_0 r_0^2}{D} \end{aligned}$$

$$\frac{A r_0 B_m}{\sin(B_m R_0 - B_m r_0)} \sin(B_m R_0) = \frac{q_0 r_0^2}{D}$$

Therefore A is obtained as

$$A = \frac{q_0 r_0 \sin(B_m R_0 - B_m r_0)}{D B_m \sin(B_m R_0)} \quad (4.45)$$

Therefore G is

$$G = A \frac{\sin(B_m r_0)}{\sin(B_m R_0 - B_m r_0)}$$

$$G = \frac{q_0 r_0 \sin(B_m r_0)}{D B_m \sin(B_m R_0)} \quad (4.46)$$

Hence Solutions are obtained as

$$\phi_I(r) = \frac{q_0 r_0 \sin(B_m R_0 - B_m r_0) \sin(B_m r)}{D B_m \sin(B_m R_0) r} \quad (4.47)$$

$$\phi_{II}(r) = \frac{q_0 r_0 \sin(B_m r_0) \sin(B_m R_0 - B_m r)}{D B_m \sin(B_m R_0) r} \quad (4.48)$$

$$k_s = \frac{S}{S + Q}$$

Where S is the total number of fission neutrons and Q is total number of source neutrons. Since the problem is consisted of two regions the boundaries and variables of integral changes

$$k_s = \frac{\vartheta \sum_f \left( \int_0^{r_0} \phi_{gI}(r) 4\pi r^2 dr + \int_{r_0}^{R_0} \phi_{gII}(r) 4\pi r^2 dr \right)}{\left( \vartheta \sum_f \left( \int_0^{r_0} \phi_{gI}(r) 4\pi r^2 dr + \int_{r_0}^{R_0} \phi_{gII}(r) 4\pi r^2 dr \right) + \int_{r_0-\delta}^{r_0+\delta} \delta(r - r_0) q_0 4\pi r^2 dr \right)}$$

$$k_s = \frac{1}{1 + \frac{\int_{r_0-\delta}^{r_0+\delta} \delta(r - r_0) q_0 r^2 dr}{\vartheta \sum_f \left( \int_0^{r_0} \phi_{gI}(r) r^2 dr + \int_{r_0}^{R_0} \phi_{gII}(r) r^2 dr \right)}} \quad (4.49)$$

To solve the first integration, integration by parts must be applied

$$\int_0^{r_0} \phi_{gI}(r) r^2 dr = \int_0^{r_0} \frac{q_0 r_0 \sin(B_m R_0 - B_m r_0) \sin(B_m r)}{D B_m \sin(B_m R_0) r} r^2 dr$$

$$\int_0^{r_0} \phi_{gI}(r) r^2 dr = \frac{q_0 r_0 \sin(B_m R_0 - B_m r_0)}{D B_m \sin(B_m R_0)} \int_0^{r_0} \sin(B_m r) r dr$$

$$\int u dv = uv - \int v du$$

$$u = r; dv = \sin(B_m r) dr; du = dr; v = -\frac{\cos(B_m r)}{B_m}$$

$$\int_0^{r_0} r \sin(B_m r) dr = -\frac{r_0 \cos(B_m r_0)}{B_m} + \int_0^{r_0} \frac{\cos(B_m r)}{B_m} dr$$

$$\begin{aligned} \int_0^{r_0} \phi_{gI}(r) r^2 dr &= \frac{q_0 r_0 \sin(B_m R_0 - B_m r_0)}{D B_m \sin(B_m R_0)} \left( \frac{\sin(B_m r_0)}{B_m^2} - \frac{r_0 \cos(B_m r_0)}{B_m} \right) \\ &= \frac{q_0 r_0 \sin(B_m R_0 - B_m r_0)}{D B_m^3 \sin(B_m R_0)} (\sin(B_m r_0) - B_m r_0 \cos(B_m r_0)) \end{aligned}$$

To solve the second integration, integration by parts must be applied

$$\int_{r_0}^{R_0} \phi_{gII}(r) r^2 dr = \int_{r_0}^{R_0} \frac{q_0 r_0 \sin(B_m r_0) \sin(B_m R_0 - B_m r)}{D B_m \sin(B_m R_0) r} r^2 dr$$

$$\int_{r_0}^{R_0} \Phi_{gII}(r) r^2 dr = \frac{q_o r_0 \sin(B_m r_0)}{D B_m \sin(B_m R_0)} \int_{r_0}^{R_0} \sin(B_m R_0 - B_m r) r dr$$

Applying integration by parts

$$\int u dv = uv - \int v du$$

$$u = r; dv = \sin(B_m R_0 - B_m r) dr; du = dr; v = \frac{\cos(B_m R_0 - B_m r)}{B_m}$$

$$\begin{aligned} \int_{r_0}^{R_0} r \sin(B_m R_0 - B_m r) dr &= \frac{R_0 \cos(0)}{B_m} - \frac{r_0 \cos(B_m R_0 - B_m r_0)}{B_m} + \int_{r_0}^{R_0} \frac{\cos(B_m R_0 - B_m r)}{B_m} dr \\ &= \frac{R_0}{B_m} - \frac{r_0 \cos(B_m R_0 - B_m r_0)}{B_m} + \frac{1}{B_m^2} [\sin(0) - \sin(B_m R_0 - B_m r_0)] \\ &= \frac{R_0}{B_m} - \frac{r_0 \cos(B_m R_0 - B_m r_0)}{B_m} - \frac{1}{B_m^2} [\sin(B_m R_0 - B_m r_0)] \\ &= \frac{R_0 B_m - r_0 B_m \cos(B_m R_0 - B_m r_0) - \sin(B_m R_0 - B_m r_0)}{B_m^2} \end{aligned}$$

$$\begin{aligned} \int_{r_0}^{R_0} \Phi_{gII}(r) r^2 dr &= \frac{q_o r_0 \sin(B_m r_0)}{D B_m^3 \sin(B_m R_0)} (R_0 B_m - r_0 B_m \cos(B_m R_0 - B_m r_0) \\ &\quad - \sin(B_m R_0 - B_m r_0)) \end{aligned}$$

Since S

$$\begin{aligned} S &= \vartheta \Sigma_f \int_0^{r_0} \Phi_{gI}(r) r^2 dr + \vartheta \Sigma_f \int_{r_0}^{R_0} \Phi_{gII}(r) r^2 dr \\ S &= \vartheta \Sigma_f \left( \frac{q_o r_0 \sin(B_m R_0 - B_m r_0)}{D B_m^3 \sin(B_m R_0)} (\sin(B_m r_0) - B_m r_0 \cos(B_m r_0)) \right. \\ &\quad \left. + \frac{q_o r_0 \sin(B_m r_0)}{D B_m^3 \sin(B_m R_0)} (R_0 B_m - r_0 B_m \cos(B_m R_0 - B_m r_0) \right. \\ &\quad \left. - \sin(B_m R_0 - B_m r_0)) \right) \end{aligned}$$

$$\begin{aligned}
S &= \vartheta \sum_f \left( \frac{-q_o r_o}{DB_m^3 \sin(B_m R_o)} (B_m r_o (\sin(B_m R_o) - B_m r_o) \cos(B_m r_o) \right. \\
&\quad \left. + \cos(B_m R_o - B_m r_o) \sin(B_m r_o)) - B_m R_o \sin(B_m r_o) \right) \\
S &= \vartheta \sum_f \left( \frac{q_o r_o}{DB_m^3 \sin(B_m R_o)} (B_m R_o \sin(B_m r_o) - B_m r_o (\sin(B_m R_o))) \right) \\
S &= \frac{\vartheta \sum_f q_o r_o}{DB_m^3} (B_m R_o \sin(B_m r_o) \csc(B_m R_o) - B_m r_o) \tag{4.50}
\end{aligned}$$

Solving the third integral for Q

Let;

$$x = B_m R_o; y = B_m r_o$$

$$Q = \int_{r_o-\delta}^{r_o+\delta} \delta(r - r_o) q_o r^2 dr = q_o r_o^2 = q_o \frac{y^2}{B_m^2} \tag{4.51}$$

Since the third integral is obtained, the coefficient can be found

$$\begin{aligned}
B_m^2 &= \frac{k_\infty - 1}{L^2} \\
S &= \frac{k_\infty q_o B_m r_o}{(k_\infty - 1) B_m^2} (B_m R_o \sin(B_m r_o) \csc(B_m R_o) - B_m r_o) \\
S &= \frac{k_\infty q_o y}{(k_\infty - 1) B_m^2} (x \sin(y) \csc(x) - y) \tag{4.52}
\end{aligned}$$

Therefore

$$\begin{aligned}
k_s &= \frac{\frac{k_\infty q_o y}{(k_\infty - 1) B_m^2} (x \sin(y) \csc(x) - y)}{\frac{k_\infty q_o y}{(k_\infty - 1) B_m^2} (x \sin(y) \csc(x) - y) + q_o \frac{y^2}{B_m^2}} \\
k_s &= \frac{\frac{k_\infty q_o y}{(k_\infty - 1)} (x \sin(y) \csc(x) - y)}{\frac{k_\infty q_o y}{(k_\infty - 1)} (x \sin(y) \csc(x) - y) + q_o y^2} \\
k_s &= \frac{k_\infty q_o (x \sin(y) \csc(x) - y)}{k_\infty q_o (x \sin(y) \csc(x) - y) + (k_\infty - 1) q_o y} \\
k_s &= \frac{k_\infty (y - x \sin(y) \csc(x))}{y - k_\infty x \sin(y) \csc(x)} \tag{4.53}
\end{aligned}$$



Now that  $k_s$  is obtained it is also possible to find  $M_s$  where as

$$\begin{aligned}
M_s &= \frac{k_s}{1 - k_s} \\
1 - k_s &= \frac{(1 - k_\infty)y}{y - k_\infty x \sin(y) \csc(x)}; \frac{1}{1 - k_s} = \frac{y - k_\infty x \sin(y) \csc(x)}{(1 - k_\infty)y} \\
M_s &= \frac{k_\infty(y - x \sin(y) \csc(x))}{y - k_\infty x \sin(y) \csc(x)} \frac{y - k_\infty x \sin(y) \csc(x)}{(1 - k_\infty)y} \\
M_s &= \frac{k_\infty}{(k_\infty - 1)} \frac{(x \sin(y) \csc(x) - y)}{y} \tag{4.54}
\end{aligned}$$

To obtain efficiency

$$\varphi^* = \frac{1 - k_{eff}}{k_{eff}} M_s$$

Where  $k_{eff}$

$$k_{eff} = \frac{k_\infty x^2}{x^2 + (k_\infty - 1)\pi^2}$$

Hence

$$\begin{aligned}
1 - k_{eff} &= \frac{x^2 + (k_\infty - 1)\pi^2 - k_\infty x^2}{x^2 + (k_\infty - 1)\pi^2} = \frac{(k_\infty - 1)(\pi^2 - x^2)}{x^2 + (k_\infty - 1)\pi^2} \\
\frac{1 - k_{eff}}{k_{eff}} &= \frac{(k_\infty - 1)(\pi^2 - x^2)}{x^2 + (k_\infty - 1)\pi^2} \frac{x^2 + (k_\infty - 1)\pi^2}{k_\infty x^2} \\
\frac{1 - k_{eff}}{k_{eff}} &= \frac{(k_\infty - 1)(\pi^2 - x^2)}{k_\infty x^2} \\
\varphi^* &= \frac{(k_\infty - 1)(\pi^2 - x^2)}{k_\infty x^2} \frac{k_\infty}{(k_\infty - 1)} \frac{(x \sin(y) \csc(x) - y)}{y} \\
\varphi^* &= \frac{(\pi^2 - x^2)(x \sin(y) \csc(x) - y)}{x^2 y} \\
\varphi^* &= \frac{(\pi^2 - (B_m R_0)^2)(B_m R_0 \sin(B_m r_0) \csc(B_m R_0) - B_m r_0)}{(B_m R_0)^2 B_m r_0} \tag{4.55}
\end{aligned}$$

### 4.3 One Group Two Region System with Flat Source in the Inner Region

To obtain a solution for a unit source, the equation must be solved for two regions that are consisted of non-multiplying region with Dirac delta source and a multiplying region without source

For the first region, there must be a homogeneous solution and a particular solution

$$-D \frac{1}{r^2} \frac{d}{dr} \left[ r^2 \frac{d\phi(r)}{dr} \right] + \Sigma_a \phi(r) = q_o \quad (4.56)$$

For General Solution

$$-D \frac{1}{r^2} \frac{d}{dr} \left[ r^2 \frac{d\phi(r)}{dr} \right] + \Sigma_a \phi(r) = 0 \quad (4.57)$$

Since

$$L^2 = \frac{D}{\Sigma_a}$$

$$\frac{1}{r^2} \frac{d}{dr} \left[ r^2 \frac{d\phi(r)}{dr} \right] - \frac{1}{L^2} \phi(r) = 0$$

Applying the transformation

$$\phi(r) = \frac{w(r)}{r}$$

$$w(r)'' - \frac{1}{L^2} w(r) = 0$$

Since the sign is minus at k constant, the solution

$$w(r) = A \sinh\left(\frac{r}{L}\right) + B \cosh\left(\frac{r}{L}\right)$$

Therefore the general solution

$$\phi(r) = \frac{A}{r} \sinh\left(\frac{r}{L}\right) + \frac{B}{r} \cosh\left(\frac{r}{L}\right) \quad (4.58)$$

For particular solution, since solution is constant the derivative part cancels

$$\phi_p \Sigma_a = q_o \quad (4.59)$$

$$\phi_p = \frac{q_o}{\Sigma_a}$$

Applying the boundary condition for central neutron flux

$$\phi(r) = \frac{A}{r} \sinh\left(\frac{r}{L}\right) + \frac{B}{r} \cosh\left(\frac{r}{L}\right)$$

For  $r \rightarrow 0$   $\phi(r) \neq \infty$  Therefore  $B = 0$

$$\phi(r) = \frac{A}{r} \sinh\left(\frac{r}{L}\right)$$

$$\phi_{gI}(r) = \frac{A}{r} \sinh\left(\frac{r}{L}\right) + \frac{q_0}{\Sigma_a} \quad (4.60)$$

For the second region which is multiplying and without source

$$-D \frac{1}{r^2} \frac{d}{dr} \left[ r^2 \frac{d\phi(r)}{dr} \right] + \Sigma_a \phi(r) - \vartheta \Sigma_f \phi(r) = 0 \quad (4.61)$$

The solution had been obtained as

$$\phi(r) = C \frac{\sin(B_m r)}{r} + D \frac{\cos(B_m r)}{r}$$

For  $r \rightarrow R_0$   $\phi(r) = 0$

$$\phi_{gII}(R_0) = C \frac{\sin(B_m R_0)}{R_0} + D \frac{\cos(B_m R_0)}{R_0} = 0$$

For that to be possible

$$C \sin(B_m R_0) + D \cos(B_m R_0) = 0 \quad (4.62)$$

$$C \tan(B_m R_0) = -D$$

$$\phi_{gII}(r) = \frac{1}{r} (C \sin(B_m r) - C \tan(B_m R_0) \cos(B_m r)) = 0$$

$$\phi_{gII}(r) = \frac{C}{r \cos(B_m R_0)} (\sin(B_m r) \cos(B_m R_0) - \sin(B_m R_0) \cos(B_m r)) = 0$$

$$\phi_{gII}(r) = \frac{C \sin(B_m R_0 - B_m r)}{r \cos(B_m R_0)}$$

$$G = C / \cos(B_m R_0)$$

$$\phi_{gII}(r) = G \frac{\sin(B_m R_0 - B_m r)}{r} \quad (4.63)$$

Two regions have boundary conditions with respect to their intersection point

$$\phi_{gI}(r_0) = \phi_{gII}(r_0) \quad (4.64)$$

$$-D_I \frac{d\phi_{gI}(r_0)}{dr} = -D_{II} \frac{d\phi_{gII}(r_0)}{dr} \quad (4.65)$$

Applying the first boundary condition and equating them for value of  $r_0$

$$\frac{A}{r_0} \sinh\left(\frac{r_0}{L}\right) + \frac{q_o}{\Sigma_a} = G \frac{\sin(B_m R_0 - B_m r_0)}{r_0}$$

Applying the second boundary condition

$$D_I \frac{d\phi_{gI}(r)}{dr} = \frac{D_I A r^{-2}}{L} \left( r \cosh\left(\frac{r}{L}\right) - L \sinh\left(\frac{r}{L}\right) \right)$$

$$D_{II} \frac{d\phi_{gII}(r)}{dr} = -D_{II} G r^{-2} (\sin(B_m R_0 - B_m r) + B_m r \cos(B_m R_0 - B_m r))$$

Equating them for value of  $r_0$

$$\begin{aligned} -D_{II} G r_0^{-2} (\sin(B_m R_0 - B_m r_0) + B_m r_0 \cos(B_m R_0 - B_m r_0)) \\ = \frac{D_I A r_0^{-2}}{L} \left( r_0 \cosh\left(\frac{r_0}{L}\right) - L \sinh\left(\frac{r_0}{L}\right) \right) \end{aligned}$$

$$\begin{aligned} D_{II} G B_m \left( \frac{\sin(B_m R_0 - B_m r_0)}{B_m} + r_0 \cos(B_m R_0 - B_m r_0) \right) \\ = \frac{D_I A}{L} \left( L \sinh\left(\frac{r_0}{L}\right) - r_0 \cosh\left(\frac{r_0}{L}\right) \right) \end{aligned}$$

$$G = \frac{D_I}{D_{II}} \frac{A \left( L \sinh\left(\frac{r_0}{L}\right) - r_0 \cosh\left(\frac{r_0}{L}\right) \right)}{L B_m \left( \frac{\sin(B_m R_0 - B_m r_0)}{B_m} + r_0 \cos(B_m R_0 - B_m r_0) \right)}$$

$$A \sinh\left(\frac{r_0}{L}\right) = G \sin(B_m R_0 - B_m r_0) - \frac{r_0 q_o}{\Sigma_a}$$

$$A \sinh\left(\frac{r_0}{L}\right) = \frac{D_I}{D_{II}} \frac{A \left( L \sinh\left(\frac{r_0}{L}\right) - r_0 \cosh\left(\frac{r_0}{L}\right) \right) \sin(B_m R_0 - B_m r_0)}{L B_m \left( \frac{\sin(B_m R_0 - B_m r_0)}{B_m} + r_0 \cos(B_m R_0 - B_m r_0) \right)} - \frac{r_0 q_o}{\Sigma_a}$$

$$A \sinh\left(\frac{r_0}{L}\right) - \frac{D_I}{D_{II}} \frac{A \left( L \sinh\left(\frac{r_0}{L}\right) - r_0 \cosh\left(\frac{r_0}{L}\right) \right) \sin(B_m R_0 - B_m r_0)}{L B_m \left( \frac{\sin(B_m R_0 - B_m r_0)}{B_m} + r_0 \cos(B_m R_0 - B_m r_0) \right)} = -\frac{r_0 q_o}{\Sigma_a}$$

$$A \left( 1 - \frac{D_I}{D_{II}} \frac{A \left( L \sinh \left( \frac{r_0}{L} \right) - r_0 \cosh \left( \frac{r_0}{L} \right) \right) \sin(B_m R_0 - B_m r_0)}{LB_m \left( \frac{\sin(B_m R_0 - B_m r_0)}{B_m} + r_0 \cos(B_m R_0 - B_m r_0) \right) \sinh \left( \frac{r_0}{L} \right)} \right) = - \frac{r_0 q_o}{\sinh \left( \frac{r_0}{L} \right) \Sigma_a}$$

$$A \left( 1 - \frac{D_I}{D_{II}} \frac{\left( L - r_0 \coth \left( \frac{r_0}{L} \right) \right)}{LB_m \left( \frac{1}{B_m} + r_0 \cot(B_m R_0 - B_m r_0) \right)} \right) = - \frac{r_0 q_o}{\sinh \left( \frac{r_0}{L} \right) \Sigma_a}$$

Therefore A is obtained

$$A = \frac{r_0 q_o}{\sinh \left( \frac{r_0}{L} \right) \Sigma_a \left( \frac{D_I}{D_{II}} \frac{\left( 1 - r_0/L \coth \left( \frac{r_0}{L} \right) \right)}{\left( 1 + r_0 B_m \cot(B_m R_0 - B_m r_0) \right)} - 1 \right)} \quad (4.66)$$

Following G can be obtained as well

$$G = \frac{D_I}{D_{II}} \frac{A \sinh \left( \frac{r_0}{L} \right) \left( 1 - r_0/L \coth \left( \frac{r_0}{L} \right) \right)}{\sin(B_m R_0 - B_m r_0) \left( 1 + r_0 B_m \cot(B_m R_0 - B_m r_0) \right)}$$

$$G = \frac{r_0 q_o}{\Sigma_a \sin(B_m R_0 - B_m r_0)} \frac{\frac{D_I}{D_{II}} \frac{\left( 1 - r_0/L \coth \left( \frac{r_0}{L} \right) \right)}{\left( 1 + r_0 B_m \cot(B_m R_0 - B_m r_0) \right)}}{\frac{D_I}{D_{II}} \frac{\left( 1 - r_0/L \coth \left( \frac{r_0}{L} \right) \right)}{\left( 1 + r_0 B_m \cot(B_m R_0 - B_m r_0) \right)} - 1} \quad (4.67)$$

Since

$$\phi_{gI}(r) = \frac{A}{r} \sinh \left( \frac{r}{L} \right) + \frac{q_o}{\Sigma_a}$$

$$\phi_{gII}(r) = G \frac{\sin(B_m R_0 - B_m r)}{r}$$

Therefore

$$\phi_{gI}(r) = \frac{r_0 q_o}{\sinh \left( \frac{r_0}{L} \right) \Sigma_a \left( \frac{D_I}{D_{II}} \frac{\left( 1 - r_0/L \coth \left( \frac{r_0}{L} \right) \right)}{\left( 1 + r_0 B_m \cot(B_m R_0 - B_m r_0) \right)} - 1 \right)} \sinh \left( \frac{r}{L} \right) + \frac{q_o}{\Sigma_a}$$

Simplifying further

$$\phi_{gI}(r) = \frac{q_o}{\Sigma_a} \left( 1 + \frac{r_o \sinh\left(\frac{r}{L}\right)}{\left(\frac{D_I}{D_{II}} \left( \frac{1 - r_o/L \coth\left(\frac{r_o}{L}\right)}{1 + r_o B_m \cot(B_m R_o - B_m r_o)} \right) - 1 \right) r \sinh\left(\frac{r_o}{L}\right)} \right)$$

Let

$$E = \frac{D_I}{D_{II}} \frac{1 - r_o/L \coth\left(\frac{r_o}{L}\right)}{1 + r_o B_m \cot(B_m R_o - B_m r_o)}$$

Hence

$$\phi_{gI}(r) = \frac{q_o}{\Sigma_a} \left( 1 + \frac{r_o \sinh\left(\frac{r}{L}\right)}{(E-1)r \sinh\left(\frac{r_o}{L}\right)} \right) \quad (4.68)$$

Likewise

$$\phi_{gII}(r)$$

$$= \frac{r_o q_o}{\sin(B_m R_o - B_m r_o) \Sigma_a} \frac{\frac{D_I}{D_{II}} \frac{(1 - r_o/L \coth\left(\frac{r_o}{L}\right))}{(1 + r_o B_m \cot(B_m R_o - B_m r_o))}}{\frac{D_I}{D_{II}} \frac{(1 - r_o/L \coth\left(\frac{r_o}{L}\right))}{(1 + r_o B_m \cot(B_m R_o - B_m r_o))} - 1} \frac{\sin(B_m R_o - B_m r)}{r}$$

Using  $E$

$$\phi_{gII}(r) = \frac{q_o}{\Sigma_a} \frac{E}{E-1} \frac{r_o \sin(B_m R_o - B_m r)}{r \sin(B_m R_o - B_m r_o)} \quad (4.69)$$

Where  $S$  is the total number of fission neutrons and  $Q$  is total number of source neutrons. Since the problem is consisted of two regions the boundaries and variables of integral changes;

$$k_s = \frac{\vartheta \Sigma_f \phi_{II} V_{II}}{\vartheta \Sigma_f \phi_{II} V_{II} + q_o V_I}$$

$$k_s = \frac{\vartheta \Sigma_f \phi_{II} (R_o^3 - r_o^3)}{\vartheta \Sigma_f \phi_{II} (R_o^3 - r_o^3) + q_o r_o^3}$$

$$k_s = \frac{1}{1 + \frac{q_o r_o^3}{\vartheta \Sigma_f \phi_{II} (R_o^3 - r_o^3)}}$$

$$\phi_{II} = \frac{\int_{r_0}^{R_0} \phi_{gII}(r) r^2 dr}{V_{II}} = \int_{r_0}^{R_0} \frac{3q_o}{(R_0^3 - r_0^3)\Sigma_a} \frac{E}{E-1} \frac{r_0 \sin(B_m R_0 - B_m r)}{r \sin(B_m R_0 - B_m r_0)} r^2 dr$$

$$\phi_{II} = \frac{3q_o r_0}{\sin(B_m R_0 - B_m r_0) (R_0^3 - r_0^3)\Sigma_a} \frac{E}{E-1} \int_{r_0}^{R_0} r \sin(B_m R_0 - B_m r) dr$$

Applying integration by parts

$$\int u dv = uv - \int v du$$

$$u = r; dv = \sin(B_m R_0 - B_m r) dr; du = dr; v = \frac{\cos(B_m R_0 - B_m r)}{B_m}$$

$$\begin{aligned} & \int_{r_0}^{R_0} r \sin(B_m R_0 - B_m r) dr \\ &= \frac{R_0 \cos(0)}{B_m} - \frac{r_0 \cos(B_m R_0 - B_m r_0)}{B_m} + \int_{r_0}^{R_0} \frac{\cos(B_m R_0 - B_m r)}{B_m} dr \end{aligned}$$

$$= \frac{R_0}{B_m} - \frac{r_0 \cos(B_m R_0 - B_m r_0)}{B_m} + \frac{1}{B_m^2} [\sin(0) - \sin(B_m R_0 - B_m r_0)]$$

$$= \frac{R_0}{B_m} - \frac{r_0 \cos(B_m R_0 - B_m r_0)}{B_m} - \frac{1}{B_m^2} [\sin(B_m R_0 - B_m r_0)]$$

$$= \frac{(R_0 B_m - r_0 B_m \cos(B_m R_0 - B_m r_0) - \sin(B_m R_0 - B_m r_0))}{B_m^2}$$

$$\phi_{II} = \frac{3q_o r_0 (R_0 B_m - r_0 B_m \cos(B_m R_0 - B_m r_0) - \sin(B_m R_0 - B_m r_0))}{B_m^2 \sin(B_m R_0 - B_m r_0) (R_0^3 - r_0^3)\Sigma_a} \frac{E}{E-1}$$

Therefore

$k_s$

$$= \frac{1}{1 + \frac{q_o r_0^2}{\vartheta \Sigma_f \frac{3q_o r_0 (R_0 B_m - r_0 B_m \cos(B_m R_0 - B_m r_0) - \sin(B_m R_0 - B_m r_0))}{B_m^2 \sin(B_m R_0 - B_m r_0) (R_0^3 - r_0^3)\Sigma_a} \frac{E}{E-1} (R_0^3 - r_0^3)}}$$

$$k_s = \frac{1}{1 + \frac{q_o r_0^2}{\vartheta \Sigma_f \frac{3q_o (R_0 B_m - r_0 B_m \cos(B_m R_0 - B_m r_0) - \sin(B_m R_0 - B_m r_0))}{B_m^2 \sin(B_m R_0 - B_m r_0) \Sigma_a} \frac{E}{E-1}}}}$$

$$k_s = \frac{1}{1 + \frac{q_0 r_0^2 (E-1) B_m^2 \sin(B_m R_0 - B_m r_0) \Sigma_a}{\vartheta \Sigma_{f3} q_0 (R_0 B_m - r_0 B_m \cos(B_m R_0 - B_m r_0) - \sin(B_m R_0 - B_m r_0)) E}} \quad (4.70)$$

$$M_s = \frac{k_s}{1 - k_s}$$

$$\varphi^* = \frac{1 - k_{eff}}{k_{eff}} M_s$$

#### 4.4 Two Group One Region Dirac Source

For the two group solution, there are two equations for criticality

$$-D_1 \nabla^2 \phi_I(r) + \Sigma_{a1} \phi_I(r) = \vartheta \Sigma_{f1} \phi_I(r) + \vartheta \Sigma_{f2} \phi_{II}(r) \quad (4.71)$$

$$-D_2 \nabla^2 \phi_{II}(r) + \Sigma_{a2} \phi_{II}(r) = \Sigma_{s2} \phi_I(r) \quad (4.72)$$

Since two equations harbor neutron flux for first and second energy groups, they can be rewritten in one equation

For the first equation

$$\frac{D_1}{\Sigma_{a1} - \vartheta \Sigma_{f1}} = M_I^2$$

$$\nabla^2 \phi_I(r) + \frac{(\vartheta \Sigma_{f1} - \Sigma_{a1})}{D_1} \phi_I(r) = -\frac{\vartheta \Sigma_{f2}}{D_1} \phi_{II}(r)$$

$$\nabla^2 \phi_I(r) + \frac{1}{M_I^2} \phi_I(r) = -\frac{\vartheta \Sigma_{f2}}{D_1} \phi_{II}(r) \quad (4.73)$$

For the second equation

$$\frac{D_2}{\Sigma_{a2}} = M_{II}^2$$

$$\nabla^2 \phi_{II}(r) - \frac{\Sigma_{a2}}{D_2} \phi_{II}(r) = -\frac{\Sigma_{s2}}{D_2} \phi_I(r)$$

$$\nabla^2 \phi_{II}(r) - \frac{1}{M_{II}^2} \phi_{II}(r) = -\frac{\Sigma_{s2}}{D_2} \phi_I(r) \quad (4.74)$$

To obtain a solution for  $\phi_I$  in the form of  $\phi_{II}$

$$\phi_I(r) = -\frac{D_2}{\Sigma_{s2}} \left( \nabla^2 \phi_{II}(r) - \frac{1}{M_{II}^2} \phi_{II}(r) \right)$$



$$\begin{aligned}\phi_I(r) &= -\frac{D_2}{\Sigma_{s2}} \nabla^2 \phi_{II}(r) + \frac{\mathfrak{D}_z \Sigma_{a2}}{\Sigma_{s2} \mathfrak{D}_z} \phi_{II}(r) \\ \phi_I(r) &= -\frac{D_2}{\Sigma_{s2}} \nabla^2 \phi_{II}(r) + \frac{\Sigma_{a2}}{\Sigma_{s2}} \phi_{II}(r)\end{aligned}\quad (4.75)$$

Constructing the elements of first equation

$$\begin{aligned}\nabla^2 \phi_I(r) &= -\frac{D_2}{\Sigma_{s2}} \nabla^4 \phi_{II}(r) + \nabla^2 \frac{\Sigma_{a2}}{\Sigma_{s2}} \phi_{II}(r) \\ \frac{1}{M_I^2} \phi_I(r) &= -\frac{D_2}{M_I^2 \Sigma_{s2}} \nabla^2 \phi_{II}(r) + \frac{\Sigma_{a2}}{M_I^2 \Sigma_{s2}} \phi_{II}(r)\end{aligned}$$

Rewriting for the first equation

$$\nabla^2 \phi_I(r) + \frac{1}{M_I^2} \phi_I(r) = -\frac{\vartheta \Sigma_{f2}}{D_1} \phi_{II}(r)$$

Therefore

$$\begin{aligned}-\frac{D_2}{\Sigma_{s2}} \nabla^4 \phi_{II}(r) + \nabla^2 \frac{\Sigma_{a2}}{\Sigma_{s2}} \phi_{II}(r) - \frac{D_2}{M_I^2 \Sigma_{s2}} \nabla^2 \phi_{II}(r) + \frac{\Sigma_{a2}}{M_I^2 \Sigma_{s2}} \phi_{II}(r) - \frac{\vartheta \Sigma_{f2}}{D_1} \phi_{II}(r) \\ = 0\end{aligned}$$

$$\begin{aligned}\nabla^4 \phi_{II}(r) - \nabla^2 \frac{\Sigma_{a2} \Sigma_{s2}}{D_2 \Sigma_{s2}} \phi_{II}(r) + \frac{\mathfrak{D}_z \Sigma_{s2}}{M_I^2 \mathfrak{D}_z \Sigma_{s2}} \nabla^2 \phi_{II}(r) - \frac{\Sigma_{a2} \Sigma_{s2}}{M_I^2 D_2 \Sigma_{s2}} \phi_{II}(r) \\ + \frac{\vartheta \Sigma_{f2} \Sigma_{s2}}{D_1 D_2} \phi_{II}(r) = 0\end{aligned}$$

$$\nabla^4 \phi_{II}(r) - \nabla^2 \frac{\Sigma_{a2}}{D_2} \phi_{II}(r) + \frac{1}{M_I^2} \nabla^2 \phi_{II}(r) - \frac{\Sigma_{a2}}{M_I^2 D_2} \phi_{II}(r) + \frac{\vartheta \Sigma_{f2} \Sigma_{s2}}{D_1 D_2} \phi_{II}(r) = 0$$

$$\nabla^4 \phi_{II}(r) - \nabla^2 \phi_{II}(r) \left( \frac{1}{M_{II}^2} - \frac{1}{M_I^2} \right) - \phi_{II}(r) \left( \frac{1}{M_I^2 M_{II}^2} - \frac{\vartheta \Sigma_{f2} \Sigma_{s2}}{D_1 D_2} \right) = 0$$

For

$$k = \frac{\vartheta \Sigma_{f2} \Sigma_{s2}}{\Sigma_{a2} (\Sigma_{a1} - \vartheta \Sigma_{f1})}$$

$$\frac{\vartheta \Sigma_{f2} \Sigma_{s2}}{D_1 D_2} = \frac{\vartheta \Sigma_{f2}}{\Sigma_{a2} M_{II}^2} \frac{\Sigma_{s2}}{M_I^2 (\Sigma_{a1} - \vartheta \Sigma_{f1})} = \frac{k}{M_I^2 M_{II}^2}$$

Hence

$$\nabla^4 \phi_{II}(r) + \nabla^2 \phi_{II}(r) \left( \frac{1}{M_{II}^2} - \frac{1}{M_I^2} \right) - \phi_{II}(r) \left( \frac{1-k}{M_I^2 M_{II}^2} \right) = 0$$

$$\phi_{II}(r) \left( \nabla^4 - \nabla^2 \left( \frac{1}{M_{II}^2} - \frac{1}{M_I^2} \right) - \left( \frac{1-k}{M_I^2 M_{II}^2} \right) \right) = 0 \quad (4.76)$$

Therefore

$$\phi_{II}(r) (\nabla^4 - \lambda^2 \nabla^2 + \mu^2 \nabla^2 - \mu^2 \lambda^2) = 0$$

$$\phi_{II}(r) (\nabla^4 - (\mu^2 + \lambda^2) \nabla^2 - \mu^2 \lambda^2)$$

$$\phi_{II}(r) (\nabla^2 + \mu^2) (\nabla^2 - \lambda^2) = 0 \quad (4.77)$$

For the case  $k > 1$

$$\phi_I(r) = AX(r) + CY(r) \quad (4.78)$$

$$(\nabla^2 + \mu^2) X = 0$$

$$(\nabla^2 - \lambda^2) Y = 0$$

$$\mu^2 = \frac{1}{2M_I^2 M_{II}^2} \left( -(M_I^2 + M_{II}^2) + \sqrt{M_I^2 + M_{II}^2 + 4(k-1)M_I^2 M_{II}^2} \right)$$

$$\lambda^2 = \frac{1}{2M_I^2 M_{II}^2} \left( (M_I^2 + M_{II}^2) + \sqrt{M_I^2 + M_{II}^2 + 4(k-1)M_I^2 M_{II}^2} \right)$$

$$\phi_{II} = S_I AX(r) + S_{II} CY(r) \quad (4.79)$$

$$S_I = \frac{\Sigma_{s2}/\Sigma_{a2}}{1+M_{II}^2\mu^2}; S_{II} = \frac{\Sigma_{s2}/\Sigma_{a2}}{1-M_{II}^2\lambda^2} \quad (4.80)$$

For  $r < r_0$

$$X(r) = \frac{\sin(\mu r)}{r}; Y(r) = \frac{\sinh(\lambda r)}{r}$$

Hence

$$\phi_I(r) = A \frac{\sin(\mu r)}{r} + C \frac{\sinh(\lambda r)}{r} \quad (4.81)$$

For  $r > r_0$

$$X(r) = A' \frac{\sin(\mu r)}{r} + C' \frac{\cos(\mu r)}{r}$$

$$Y(r) = A'' \frac{\sinh(\lambda r)}{r} + C'' \frac{\cosh(\lambda r)}{r}$$

$$X(R_0) = A' \frac{\sin(\mu R_0)}{R_0} + C' \frac{\cos(\mu R_0)}{R_0} = 0$$

$$C' = -A' \frac{\sin(\mu R_0)}{\cos(\mu R_0)} \quad (4.82)$$

$$X(r) = \frac{A'}{r} \left( \sin(\mu r) - \frac{\sin(\mu R_0)}{\cos(\mu R_0)} \cos(\mu r) \right)$$

$$X(r) = \frac{A'}{r \cos(\mu R_0)} (\sin(\mu r) \cos(\mu R_0) - \sin(\mu R_0) \cos(\mu r))$$

$$X(r) = \frac{-A'}{r \cos(\mu R_0)} \sin(\mu R_0 - \mu r)$$

$$\tilde{A} = \frac{-A'}{\cos(\mu R_0)} \quad (4.83)$$

$$X(r) = \frac{\tilde{A}}{r} \sin(\mu R_0 - \mu r)$$

$$Y(R_0) = A'' \frac{\sinh(\lambda R_0)}{R_0} + C'' \frac{\cosh(\lambda R_0)}{R_0} = 0$$

$$C'' = -A'' \frac{\sinh(\lambda R_0)}{\cosh(\lambda R_0)} \quad (4.84)$$

$$Y(r) = \frac{A''}{r} \left( \sinh(\lambda r) - \frac{\sinh(\lambda R_0)}{\cosh(\lambda R_0)} \cosh(\lambda r) \right)$$

$$Y(r) = \frac{-A''}{r \cosh(\lambda R_0)} \sinh(\lambda R_0 - \lambda r)$$

$$\tilde{A} = \frac{-A''}{\cosh(\lambda R_0)} \quad (4.85)$$

$$Y(r) = \frac{\tilde{A}}{r} \sinh(\lambda R_0 - \lambda r)$$

For  $r < r_0$

$$\phi_I(r) = A \frac{\sin(\mu r)}{r} + C \frac{\sinh(\lambda r)}{r} \quad (4.86)$$

$$\phi_{II}(r) = S_I A \frac{\sin(\mu r)}{r} + S_{II} C \frac{\sinh(\lambda r)}{r} \quad (4.87)$$

For  $r > r_0$

$$\phi_I(r) = \tilde{A} \frac{\sin(\mu R_0 - \mu r)}{r} + \tilde{C} \frac{\sinh(\lambda R_0 - \lambda r)}{r} \quad (4.88)$$

$$\phi_{II}(r) = S_I \tilde{A} \frac{\sin(\mu R_0 - \mu r)}{r} + S_{II} \tilde{C} \frac{\sinh(\lambda R_0 - \lambda r)}{r} \quad (4.89)$$

Derivatives for  $r < r_0$

$$\frac{d\phi_I(r)}{dr} = \frac{A}{r^2} (\mu r \cos(\mu r) - \sin(\mu r)) + \frac{C}{r^2} (\lambda r \cosh(\lambda r) - \sinh(\lambda r))$$

$$\frac{d\phi_{II}(r)}{dr} = \frac{S_I A}{r^2} (\mu r \cos(\mu r) - \sin(\mu r)) + \frac{S_{II} C}{r^2} (\lambda r \cosh(\lambda r) - \sinh(\lambda r))$$

Derivatives for  $r > r_0$

$$\begin{aligned} \frac{d\phi_I(r)}{dr} = & -\frac{\tilde{A}}{r^2} (\mu r \cos(\mu R_0 - \mu r) + \sin(\mu R_0 - \mu r)) \\ & - \frac{\tilde{C}}{r^2} (\lambda r \cosh(\lambda R_0 - \lambda r) + \sinh(\lambda R_0 - \lambda r)) \end{aligned}$$

$$\begin{aligned} \frac{d\phi_{II}(r)}{dr} = & -\frac{\tilde{A} S_I}{r^2} (\mu r \cos(\mu R_0 - \mu r) + \sin(\mu R_0 - \mu r)) \\ & - \frac{\tilde{C} S_{II}}{r^2} (\lambda r \cosh(\lambda R_0 - \lambda r) + \sinh(\lambda R_0 - \lambda r)) \end{aligned}$$

Applying Boundary Conditions for Interface

$$\phi_I(r_0^-) = \phi_I(r_0^+)$$

$$A \sin(\mu r_0) + C \sinh(\lambda r_0) = \tilde{A} \sin(\mu R_0 - \mu r_0) + \tilde{C} \sinh(\lambda R_0 - \lambda r_0)$$

$$\phi_{II}(r_0^-) = \phi_{II}(r_0^+)$$

$$S_I A \sin(\mu r_0) + S_{II} C \sinh(\lambda r_0) = S_I \tilde{A} \sin(\mu R_0 - \mu r_0) + S_{II} \tilde{C} \sinh(\lambda R_0 - \lambda r_0)$$

$$\frac{d\phi_I(r)}{dr} \Big|_{r_0^+} = \frac{d\phi_I(r)}{dr} \Big|_{r_0^-} - \frac{q_0}{D_1}$$

$$\begin{aligned} A(\mu r_0 \cos(\mu r_0) - \sin(\mu r_0)) + C(\lambda r_0 \cosh(\lambda r_0) - \sinh(\lambda r_0)) - \frac{r_0^2 q_0}{D_1} \\ = \tilde{A}(\mu r_0 \cos(\mu R_0 - \mu r_0) + \sin(\mu R_0 - \mu r_0)) \\ - \tilde{C}(\lambda r_0 \cosh(\lambda R_0 - \lambda r_0) + \sinh(\lambda R_0 - \lambda r_0)) \end{aligned}$$

$$\frac{d\phi_{II}(r)}{dr} \Big|_{r_0^+} = \frac{d\phi_{II}(r)}{dr} \Big|_{r_0^-}$$

$$\begin{aligned} & S_I A(\mu r_0 \cos(\mu r_0) - \sin(\mu r_0)) + S_{II} C(\lambda r_0 \cosh(\lambda r_0) - \sinh(\lambda r_0)) \\ &= -\tilde{A} S_I(\mu r_0 \cos(\mu R_0 - \mu r_0) + \sin(\mu R_0 - \mu r_0)) \\ & \quad - \tilde{C} S_{II}(\lambda r_0 \cosh(\lambda R_0 - \lambda r_0) + \sinh(\lambda R_0 - \lambda r_0)) \end{aligned}$$

Applying the values to the matrix for the fast dirac delta source

$$\begin{bmatrix} \sin(\mu r_0) & \sinh(\lambda r_0) & -\sin(\mu R_0 - \mu r_0) & -\sinh(\lambda R_0 - \lambda r_0) \\ S_I \sin(\mu r_0) & S_{II} \sinh(\lambda r_0) & -S_I \sin(\mu R_0 - \mu r_0) & -S_{II} \sinh(\lambda R_0 - \lambda r_0) \\ \mu r_0 \cos(\mu R_0 - \mu r_0) + \sin(\mu R_0 - \mu r_0) & \lambda r_0 \cosh(\lambda r_0) - \sinh(\lambda r_0) & \mu r_0 \cos(\mu R_0 - \mu r_0) + \sin(\mu R_0 - \mu r_0) & \lambda r_0 \cosh(\lambda R_0 - \lambda r_0) + \sinh(\lambda R_0 - \lambda r_0) \\ S_I(\mu r_0 \cos(\mu R_0 - \mu r_0) + \sin(\mu R_0 - \mu r_0)) & S_{II}(\lambda r_0 \cosh(\lambda r_0) - \sinh(\lambda r_0)) & S_I(\mu r_0 \cos(\mu R_0 - \mu r_0) + \sin(\mu R_0 - \mu r_0)) & S_{II}(\lambda r_0 \cosh(\lambda R_0 - \lambda r_0) + \sinh(\lambda R_0 - \lambda r_0)) \end{bmatrix}$$

$$\begin{bmatrix} A \\ C \\ \tilde{A} \\ \tilde{C} \end{bmatrix} = \begin{bmatrix} 0 \\ 0 \\ r_0^2 q_0 \\ D_1 \\ 0 \end{bmatrix}$$

Therefore the coefficients

$$A = -\frac{S_{II} r_0 q_0 \csc(\mu r_0) \sin(\mu R_0 - \mu r_0)}{\mu D_1 (S_I - S_{II})} \quad (4.90)$$

$$\tilde{A} = -\frac{S_{II} r_0 q_0 \csc(\mu r_0) \sin(\mu r_0)}{\mu D_1 (S_I - S_{II})} \quad (4.91)$$

$$C = \frac{S_I r_0 q_0 \operatorname{csch}(\lambda R_0) \sinh(\lambda R_0 - \lambda r_0)}{\lambda D_1 (S_I - S_{II})} \quad (4.92)$$

$$\tilde{C} = -\frac{S_I r_0 q_0 \operatorname{csch}(\lambda R_0) \sinh(\lambda r_0)}{\lambda D_1 (S_I - S_{II})} \quad (4.93)$$

Since coefficients are obtained  $k_s$  can be obtained

$$k_s = \frac{S}{S + Q}$$

For the sake of practicality

$$A = a \csc(\mu r_0) \sin(\mu R_0 - \mu r_0)$$

$$\tilde{A} = \tilde{a} \csc(\mu r_0) \sin(\mu r_0)$$

$$C = c \operatorname{csch}(\lambda R_0) \sinh(\lambda R_0 - \lambda r_0)$$

$$\tilde{C} = \tilde{c} \operatorname{csch}(\lambda R_0) \sinh(\lambda r_0)$$

$$\phi_I(r) = \left[ \begin{array}{l} \frac{A \sin(\mu r)}{r} + \frac{C \sinh(\lambda r_0)}{r} \text{ for } 0 < r < r_0 \\ \frac{\tilde{A} \sin(\mu R_0 - \mu r)}{r} + \frac{\tilde{C} \sinh(\lambda R_0 - \lambda r)}{r} \text{ for } r_0 < r < R_0 \end{array} \right]$$

$$\phi_{II}(r) = \left[ \begin{array}{l} \frac{S_I A \sin(\mu r)}{r} + \frac{S_{II} C \sinh(\lambda r_0)}{r} \text{ for } 0 < r < r_0 \\ \frac{S_I \tilde{A} \sin(\mu R_0 - \mu r)}{r} + \frac{S_{II} \tilde{C} \sinh(\lambda R_0 - \lambda r)}{r} \text{ for } r_0 < r < R_0 \end{array} \right]$$

$$S = (\vartheta \sum_{f1} \phi_I + \vartheta \sum_{f2} \phi_{II}) \frac{4\pi R_0^3}{3}$$

$$Q = 4\pi q_0 R_0^2$$

$$\phi_I = \int_0^{R_0} \phi_I(r) 4\pi r^2 dr \frac{1}{\frac{4\pi R_0^3}{3}} = \frac{3}{R_0^3} \int_0^{R_0} \phi_I(r) r^2 dr$$

$$\phi_I = \frac{3}{R_0^3} \left( A \int_0^{r_0} r \sin(\mu r) dr + C \int_0^{r_0} r \sinh(\lambda r) dr + \tilde{A} \int_{r_0}^{R_0} r \sin(\mu R_0 - \mu r) dr + \tilde{C} \int_{r_0}^{R_0} r \sinh(\lambda R_0 - \lambda r) dr \right)$$

$$\phi_I = \frac{3}{R_0^3} \left( A \left( \frac{\sin(\mu r_0) - \mu r_0 \cos(\mu r_0)}{\mu^2} \right) + C \left( \frac{\lambda r_0 \cosh(\lambda r_0) - \sinh(\lambda r_0)}{\lambda^2} \right) + \tilde{A} \left( \frac{\mu R_0 - \sin(\mu R_0 - \mu r_0) - \mu r_0 \cos(\mu R_0 - \mu r_0)}{\mu^2} \right) + \tilde{C} \left( \frac{\lambda r_0 \cosh(\lambda R_0 - \lambda r_0) - \lambda r_0 + \sinh(\lambda R_0 - \lambda r_0)}{\lambda^2} \right) \right)$$

$$\phi_{II} = \frac{3}{R_0^3} \left( A S_I \int_0^{r_0} r \sin(\mu r) dr + C S_{II} \int_0^{r_0} r \sinh(\lambda r) dr + \tilde{A} S_I \int_{r_0}^{R_0} r \sin(\mu R_0 - \mu r) dr + \tilde{C} S_{II} \int_{r_0}^{R_0} r \sinh(\lambda R_0 - \lambda r) dr \right)$$

$$\phi_I = \frac{3}{R_0^3} \left( A S_I \left( \frac{\sin(\mu r_0) - \mu r_0 \cos(\mu r_0)}{\mu^2} \right) + C S_{II} \left( \frac{\lambda r_0 \cosh(\lambda r_0) - \sinh(\lambda r_0)}{\lambda^2} \right) + \tilde{A} S_I \left( \frac{\mu R_0 - \sin(\mu R_0 - \mu r_0) - \mu r_0 \cos(\mu R_0 - \mu r_0)}{\mu^2} \right) + \tilde{C} S_{II} \left( \frac{\lambda r_0 \cosh(\lambda R_0 - \lambda r_0) - \lambda r_0 + \sinh(\lambda R_0 - \lambda r_0)}{\lambda^2} \right) \right)$$

Hence

$$k_s = \frac{(\vartheta \Sigma_{f1} \phi_I + \vartheta \Sigma_{f2} \phi_{II}) \frac{4\pi R_0^3}{3}}{(\vartheta \Sigma_{f1} \phi_I + \vartheta \Sigma_{f2} \phi_{II}) \frac{4\pi R_0^3}{3} + 4\pi q_0 R_0^2} \quad (4.94)$$

$$M_s = \frac{k_s}{1 - k_s}$$

$$\varphi^* = \frac{1 - k_{eff}}{k_{eff}} M_s$$





## 5. MATHEMATICA MODELS FOR BENCHMARK SOLUTIONS

### 5.1 One Group One Region Flat Source

Plotting the analytical solution for  $k_{eff}$  and  $k_s$  for dimensionless system ( $x = B_m R_0$ ), it can be observed that at  $x=0$  and criticality level, just as  $k_{eff}$  and  $k_s$  values are at 0 and 1 respectively.  $k_\infty$  is 1.03 (For nuclear parameters refer 6.1. One Group One Region Flat Source).

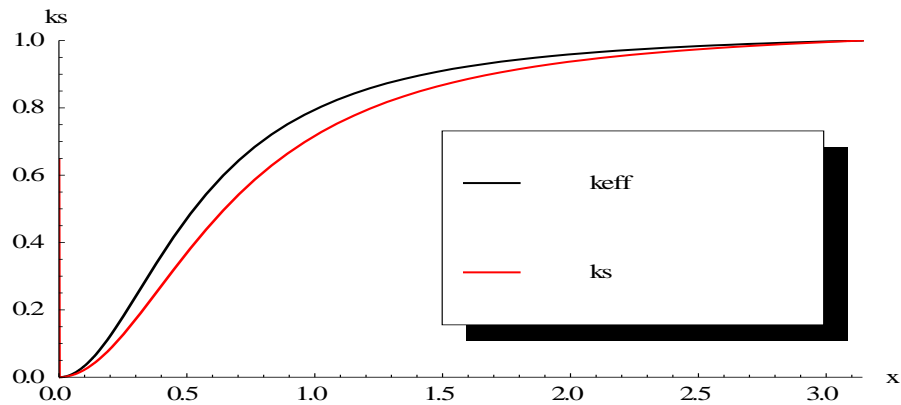


**Figure 5.1 :** One group one region flat source change of  $k_{eff}$  and  $k_s$  with radius.

Plotting the analytical solution for  $M_s$  for dimensionless system ( $x = B_m R_0$ );

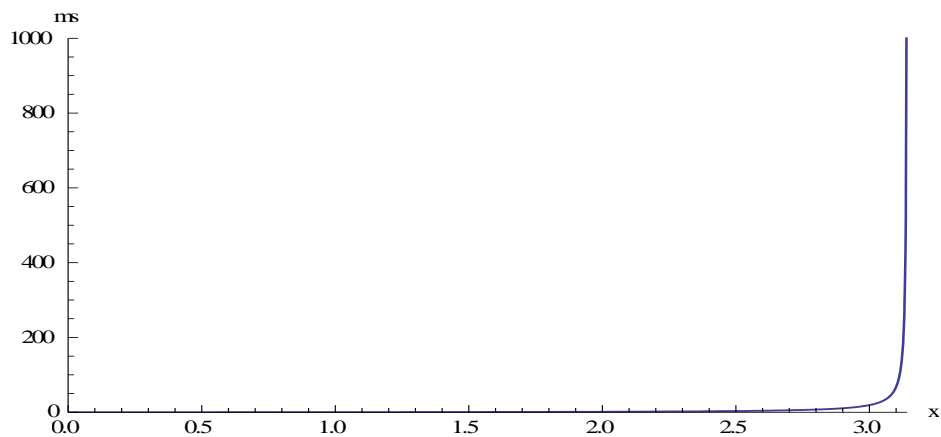


**Figure 5.2 :** One group one region flat source change of  $M_s$  with  $x$ .

Plotting the analytical solution for  $\varphi^*$  for dimensionless system ( $x = B_m R_0$ );

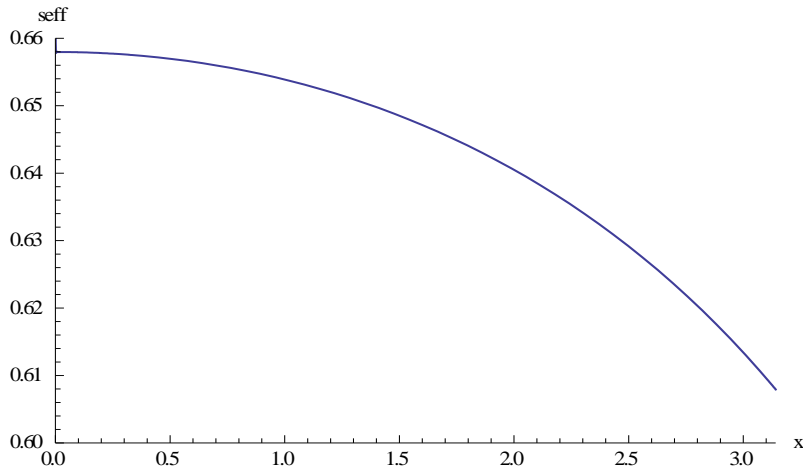


**Figure 5.3 :** One group one region flat source change of  $\varphi^*$  with x.

With one region flat source, as dimensionless radius increases source efficiency decreases. . Even though at first inspection this seems like an unexpected result, it is only natural. Since source neutrons are produced at every radial position with equal probability, the increase in the system radius, leads to an increase in the fraction of source neutrons that escape from the system without causing fission. Thus source efficiency drops.

### 5.2 One Group One Region Dirac Source

Plotting the analytical solution for  $k_{eff}$  and  $k_s$  with respect to dimensionless system ( $x = B_m R_0$ ); it can be observed that at  $x=0$  and at criticality level, both  $k_{eff}$  and  $k_s$  values are 0 and 1 respectively.  $k_\infty$  is 1.03. Dirac Delta Source is at  $0.75 x = 3\pi/4$  (For nuclear parameters refer 6.2. One Group One Region Dirac Source)

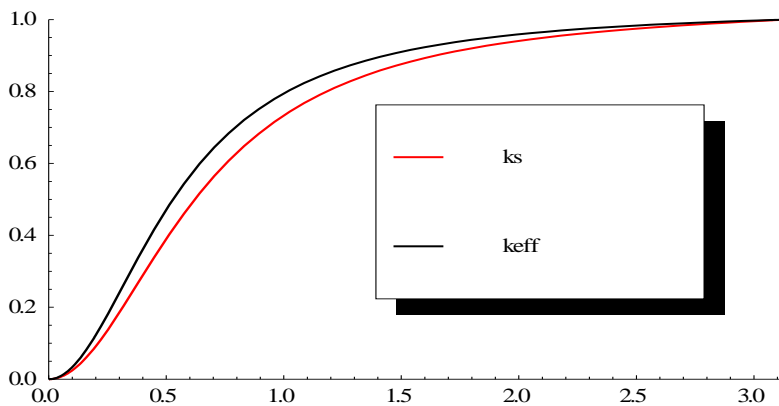


**Figure 5.4 :** One group one region Dirac source change of  $k_{eff}$  and  $k_s$  with x.

Plotting  $M_s$  with respect to dimensionless system

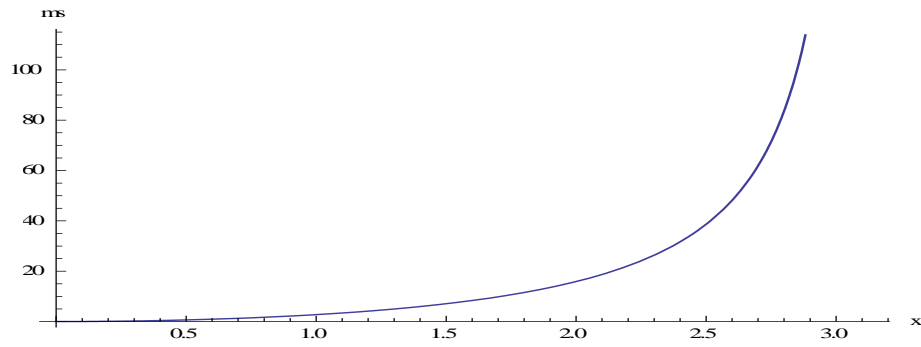


**Figure 5.5 :** One group one region Dirac source change of  $M_s$  with  $x$ .

Plotting the analytical solution for  $\varphi^*$  (seff),with respect to dimensionless source position ( $y = B_m r_0$ )

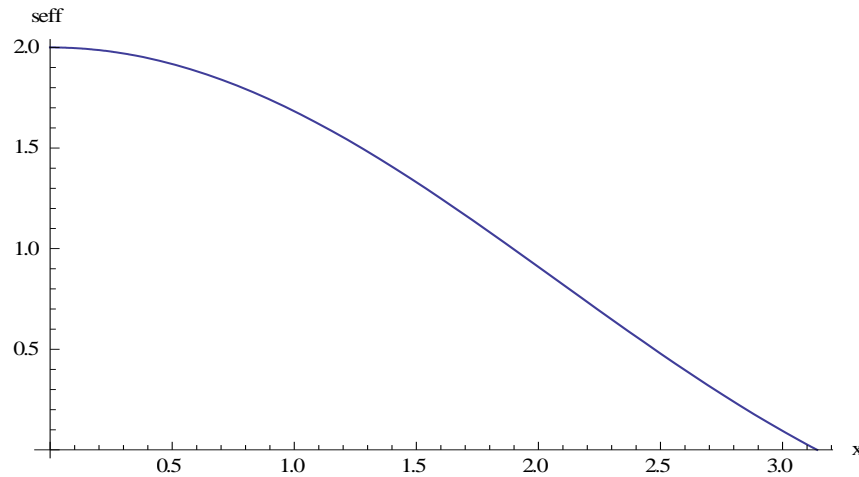


**Figure 5.6 :** One group one region Dirac source change of  $\varphi^*$  with  $y$ .

The system is chosen, has dimensions that corresponds almost to criticality, in which we have a very slightly subcritical system. From the figure, it is evident that maximizing source efficiency requires that we place the Dirac source at the center. Since the relative importance of the source is at a maximum when it is placed at the center, the source efficiency reaches its maximum value as expected.

### 5.3 One Group Two Region System With Flat Source In the Inner Region

Plotting the analytical solution for  $k_{eff}$  and  $k_s$  as a function of system radius ( $R_0$  in cm), it can be observed that at beginning and criticality level, just as  $k_{eff}$  and  $k_s$  values are at 0 and 1 respectively. Source region radius is  $r_0 = 4.1745$

(For nuclear parameters refer 6.3. One Group Two Region System with Flat Source in the Inner Region)

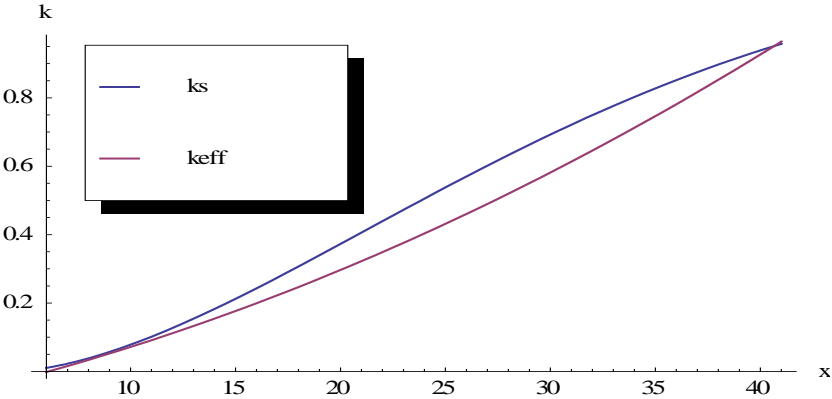


**Figure 5.7 :** One group two region with flat source in the first region change of  $k_{eff}$  and  $k_s$  with  $R_0$

Plotting the analytical solution for  $M_s$  with respect to system outer radius ( $R_0$  in cm),

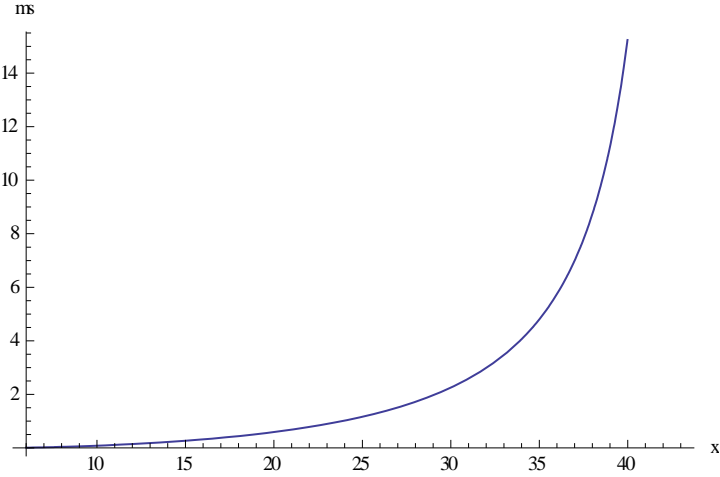


**Figure 5.8 :** One group two region with flat source in the first region change of  $M_s$  with  $R_0$

Plotting the analytical solution for  $\varphi^*$  with system outer radius ( $R_0$  in cm).

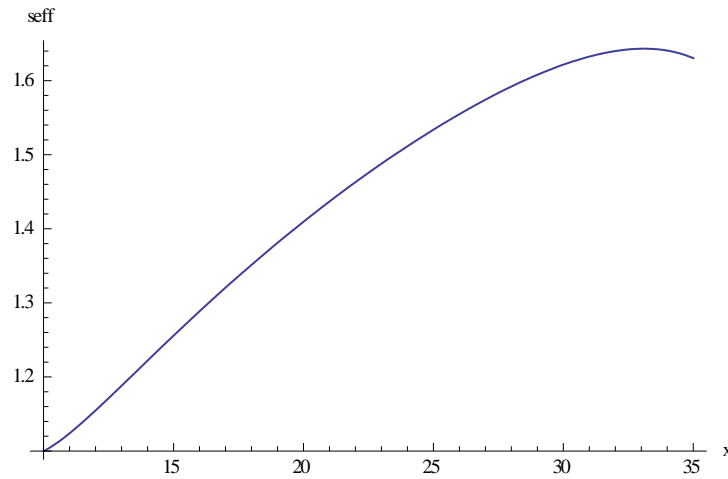


**Figure 5.9 :** One group two region with flat source in the first region change of  $\varphi^*$  with  $R_0$

Naturally as blanket area radius of the system increases, source efficiency increases proportionally.

#### 5.4 Two Group One Region Dirac Source

Plotting the analytical solution for  $k_{eff}$ ,  $tk_s$  and  $k_s$  for radius ( $x$ ), it can be observed that at beginning and criticality level, just as,  $tk_s$  and  $k_s$  values are at 0 and 1 and source at the center respectively.  $k_s$  and  $tk_s$  refer to the values of the subcritical multiplication factor when the Dirac delta source is in the fast and thermal groups, respectively. (For nuclear parameters, refer 6.4.Two Group One Region Dirac Source).

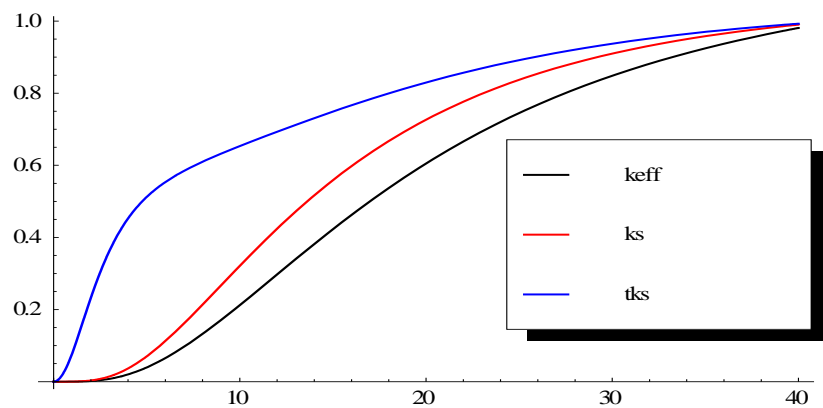


**Figure 5.10 :** Two group one region Dirac source change of  $k_{eff}, tk_s$  and  $k_s$  with  $R_0$  ( $r_0$  is placed at  $R_0/2$ ).

Considering the plot of  $tk_s$  and  $k_s$ ,  $tk_s$  is always greater than  $k_s$ , since the thermal neutrons have more capacity to cause fissions than the fast neutrons.

Plotting the analytical solution for  $M_s$  with system outer radius ( $R_0$  in cm).

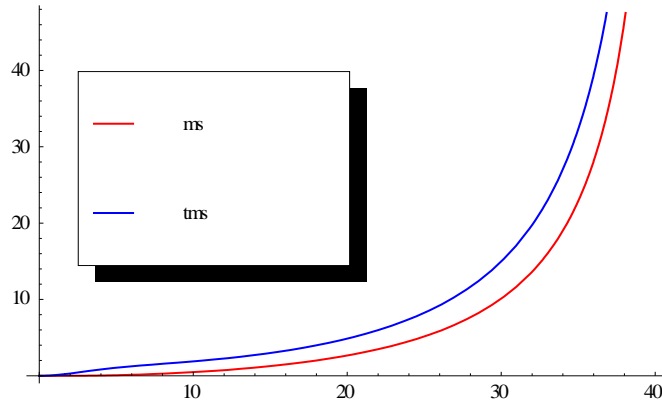


**Figure 5.11 :** Two group one region Dirac source change of  $M_s, tM_s$  with  $R_0$ .

Variation of,  $tk_s$  and  $k_s$  with respect to source position ( $r_0$  in cm)

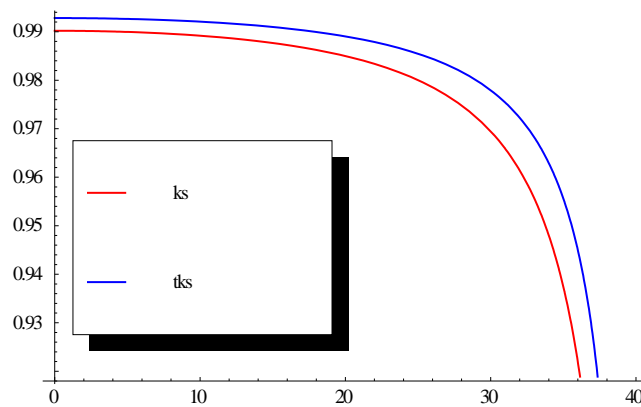


**Figure 5.12 :** Two group one region Dirac source region change of  $tk_s, k_s$  with source position  $r_0$ .

Plotting the analytical solution for  $\varphi^*, t\varphi^*$  with respect to source position ( $r_0$  in cm)

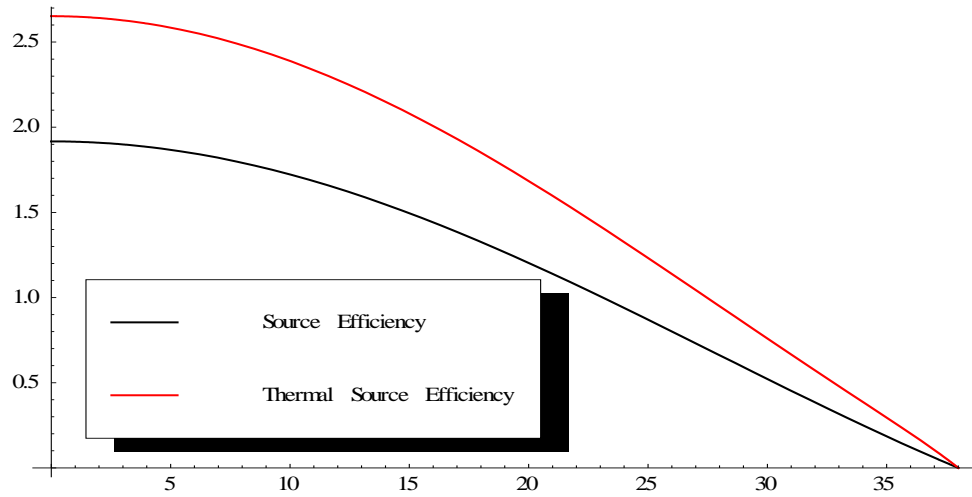


**Figure 5.13 :** Two Group One Region Dirac Source Region change of  $\varphi^*$ ,  $t\varphi^*$  with respect to source position  $r_0$ .

Relation of source position and source efficiency is displayed at the figure above. As source is moved towards the boundary of the core, source efficiency drops drastically.





## 6. COMPARISON OF ANALYTICAL AND NUMERICAL RESULTS

### 6.1 One Group One Region Flat Source

For one group one region flat source problem the finite difference multi group diffusion code DIFSP (A.Özgener, 2012) model is used with a 1000 node mesh and unit source being at a position of every given node.

**Table 6.1** : One Group One Region Flat Source Numerical Analytical Comparison.

	<i>Numerical</i>	<i>Analytical</i>	<i>Error%</i>
$D(\text{cm})$	5	5	
$\Sigma_a (1/\text{cm})$	0.1	0.1	
$\vartheta\Sigma_f(1/\text{cm})$	0.103	0.103	
$\Sigma_f(1/\text{cm})$	0.0429	0.0429	
$k_\infty$	1.03	1.03	
$B_m$	0.0244948974278	0.0244948974278	
$R_0(\text{cm})$	96.19123725999	96.19123725999	
$x = B_m R_0$	1.875112	1.875112	
$k_s$	0.92431651772	0.924316	0.0001%
$k_{eff}$	0.950000036105	0.95000002	0.0000%
$M_s$	12.2129226869	12.2129	0.0002%
$\varphi^*$	0.642784915989	0.642784	0.0001%

### 6.2 One Group One Region Dirac Source

For One Group One Region Dirac Source problem, the finite difference multi group diffusion code DIFSP (A.Özgener, 2012) model was used with a 1200 node mesh and unit source being at a position of every 800th node.

**Table 6.2 : One Group One Region Dirac Source Numerical Analytical Comparison.**

	<i>Numerical</i>	<i>Analytical</i>	<i>Error%</i>
$D$	5	5	
$\Sigma_a(1/cm)$	0.1	0.1	
$\vartheta\Sigma_f(1/cm)$	0.103	0.103	
$\Sigma_f(1/cm)$	0.0429	0.0429	
$k_\infty$	1.03	1.03	
$B_m$	0.0244948974278	0.0244948974278	
$r_0(cm)$	64.127	64.127	
$R_0(cm)$	96.19123725999	96.19123725999	
$y = B_m r_0$	1.570784	1.570784	
$x = B_m R_0$	2.356194	2.356194	
$k_s$	0.974744	0.974683	0.006%
$k_{eff}$	0.9778481	0.977848	0.000%
$M_s$	38.5951	38.4992	0.248%
$\phi^*$	0.874322	0.872151	0.248%

### 6.3 One Group Two Region System with Flat Source in the Inner Region

For One Group Two Region with Flat Source in the First Region problem the finite difference multi group diffusion code DIFSP (A.Özgener, 2012) model was used with a 480 node mesh and unit source having radius value of 4.1745 cm

**Table 6.3 :** One Group Two Region with Flat Source in the First Region Numerical Analytical Comparison.

	<i>Numerical Data</i>	<i>Analytical</i>	<i>Error%</i>
$D_I(\text{cm})$	2.08018	2.08018	
$D_{II}(\text{cm})$	1.81454	1.81454	
$\Sigma_{aI}(\text{1/cm})$	0.0177676	0.0177676	
$\Sigma_{aII}(\text{1/cm})$	0.00469138	0.00469138	
$\vartheta\Sigma_{fI}(\text{1/cm})$	0	0	
$\vartheta\Sigma_{fII}(\text{1/cm})$	0.0142548	0.0142548	
$\Sigma_{fI}(\text{1/cm})$	0	0	
$\Sigma_{fII}(\text{1/cm})$	0.0059395	0.0059395	
$k_\infty$	1.03	1.03	
$B_{mII}$	0.072598	0.0244948974278	
$L_I(\text{cm}^2)$	10.82022	10.82022	
$r_0(\text{cm})$	4.1745	4.1745	
$R_0(\text{cm})$	42	42	
$k_s$	0.975987274173	0.975986	0.0001%
$k_{eff}$	0.9556117031549	0.9556117031549	0.0000%
$M_s$	40.64458492715	40.6432	0.0004%
$\varphi^*$	1.88794663662552	1.8879551692259	0.0005%

#### 6.4 Two Group One Region Dirac Source

For Two Group One Region Dirac Source the finite difference multi group diffusion code DIFSP (A.Özgener, 2012) model was used with a 500 node mesh and unit source being at a position of 250th node.

**Table 6.4 :** Two Group One Region Dirac Source In the First Region Numerical Analytical Comparison.

	<i>Numerical Data</i>	<i>Analytical</i>	<i>Error%</i>
$D_1(\text{cm})$	1.2105	1.2105	
$D_2(\text{cm})$	0.21958	0.21958	
$\Sigma_{a1}(\text{1/cm})$	0.033338	0.033338	
$\Sigma_{a2}(\text{1/cm})$	0.05579	0.05579	
$\Sigma_{s21}(\text{1/cm})$	0.0295616	0.0295616	
$\vartheta\Sigma_{f1}(\text{1/cm})$	0	0	
$\vartheta\Sigma_{f2}(\text{1/cm})$	0.11772	0.11772	
$\Sigma_{f1}(\text{1/cm})$	0	0	
$\Sigma_{f2}(\text{1/cm})$	0.04864	0.04864	
$k_\infty$	1.21975	1.21975	
$B_m$	0.531073	0.531073	
$r_0(\text{cm})$	12	12	
$R_0(\text{cm})$	24	24	
$k_s$	0.764540621248	0.763095	0.18908%
$tk_s$	0.850309992983	0.8492868812705	0.12032%
$k_{eff}$	0.7202643559899	0.7202641806754	0.00002%
$M_s$	3.24701706	3.221101	0.79815%
$\varphi^*$	1.2610736636160	1.25101	0.79806%

## 7. SOURCE EFFICIENCY

### 7.1 Target Radius and Source Efficiency

To observe the variation of source efficiency radius with respect to target, numerical solutions are obtained for two region system, values below were obtained, while  $k_{eff}$  is kept constant at the value of 0.95. Inner region is the target region with a flat source and outer region is the blanket region. Four Group two region finite difference multi group diffusion code DIFSP (A.Özgener, 2012) model was used with a 500 node mesh and a four energy group model. Nuclear parameters are listed below.

**Table 7.1:** Nuclear Parameters for 7.Source Efficiency.

	Values		Values
$D_{I1}(cm)$	2.09	$\Sigma_{aII4}(1/cm)$	0.03151
$D_{I2}(cm)$	1.66	$\vartheta\Sigma_{fI1}(1/cm)$	0
$D_{I3}(cm)$	1.08	$\vartheta\Sigma_{fI2}(1/cm)$	0
$D_{I4}(cm)$	0.64	$\vartheta\Sigma_{fI3}(1/cm)$	0
$D_{II1}(cm)$	1.84	$\vartheta\Sigma_{fI4}(1/cm)$	0
$D_{II2}(cm)$	1.64	$\vartheta\Sigma_{fII1}(1/cm)$	0.013302124
$D_{II3}(cm)$	0.989	$\vartheta\Sigma_{fII2}(1/cm)$	0.023409464
$D_{II4}(cm)$	0.878	$\vartheta\Sigma_{fII3}(1/cm)$	0.02015619
$\Sigma_{aI1}(1/cm)$	0.018138	$\vartheta\Sigma_{fII4}(1/cm)$	0.049034
$\Sigma_{aI2}(1/cm)$	0.01247	$\Sigma_{sI21}(1/cm)$	0.000238
$\Sigma_{aI3}(1/cm)$	0.0158	$\Sigma_{sI31}(1/cm)$	0.00137
$\Sigma_{aI4}(1/cm)$	0.0351	$\Sigma_{sI41}(1/cm)$	0.0022
$\Sigma_{aII1}(1/cm)$	0.0039491	$\Sigma_{sII21}(1/cm)$	0.0000121
$\Sigma_{aII2}(1/cm)$	0.0118671	$\Sigma_{sII31}(1/cm)$	0.0000571
$\Sigma_{aII3}(1/cm)$	0.010715	$\Sigma_{sII41}(1/cm)$	0.000105

The  $k_{eff}$  is kept at constant value of 0.95. To render this possible  $R_0$  (system radius) and  $r_0$  (target radius) are modified.

**Table 7.2:** Target Radius and Source Efficiency Comparison.

$r_0(cm)$	$R_0(cm)$	$k_{eff}$	$k_s$	$M_s$	$\varphi^*$	$P(Watt)$
<b>0.0625</b>	40.97193	0.949999521722	0.972554259247849	35.43553	1.865046461756720	0.000000000002973794654
<b>0.125</b>	40.97195	0.949999860222	0.972552357507547	35.43300	1.864900303429520	0.0000000000023788661686
<b>0.25</b>	40.97203	0.950000186708	0.972544338785647	35.42236	1.864327453221380	0.0000000000190252110540
<b>0.5</b>	40.97256	0.949999569168	0.972511675905656	35.37908	1.862073843628670	0.0000000001520156208195
<b>1</b>	40.97695	0.950000083236	0.972386511688772	35.21419	1.853374959330470	0.0000000012104544876905
<b>3</b>	41.09973	0.949999919974	0.971196538495191	33.71805	1.774637169845170	0.0000000312939527171478
<b>5</b>	41.50745	0.950000082635	0.969215407120668	31.48378	1.657038268223480	0.0000001352897354678510
<b>10</b>	43.98530	0.950000493715	0.962663259337411	25.78327	1.357000097155880	0.0000008868112461472930
<b>15</b>	47.91340	0.949999960229	0.955194027217932	21.31845	1.122024784312170	0.0000024762530457723800
<b>20</b>	52.50733	0.950000250319	0.947187747203483	17.93500	0.943942387266174	0.0000049404222330101200
<b>25</b>	57.36890	0.949999584802	0.938747917418254	15.32598	0.806637340626208	0.0000082481270283522400
<b>30</b>	62.33300	0.950019943309	0.930021062140552	13.29001	0.699180745204809	0.0000123617689945867000
<b>35</b>	67.33235	0.950000024077	0.921041235502779	11.66484	0.613938556877638	0.0000172316240579757000
<b>40</b>	72.34385	0.949999790016	0.911990962480583	10.36247	0.545395539895960	0.0000228518339700811000
<b>45</b>	77.35773	0.949987443124	0.902897031428666	9.29835	0.489516022592566	0.0000291974291961845000
<b>50</b>	82.37085	0.950000050483	0.893882854551522	8.42355	0.443344153573524	0.0000362847721010127000
<b>60</b>	92.39226	0.949999734183	0.876048187907571	7.06765	0.371983729897443	0.0000526105255691546000
<b>70</b>	102.40790	0.950000401408	0.858668169665760	6.07555	0.319762926310529	0.0000718190844977592000
<b>90</b>	122.42800	0.950000219044	0.825510540299350	4.73101	0.248999125163749	0.0001188673992171600000
<b>110</b>	142.43960	0.950000440233	0.794553532900184	3.86745	0.203548009404734	0.0001774179867009440000

---

Table 7.2 (Continued)

<b>130</b>	162.44635	0.949999613997	0.765688459594175	3.26782	0.171992041147492	0.0002474528603790480000
<b>150</b>	182.45005	0.949999922556	0.738762212196719	2.82793	0.148838670757888	0.0003289673028434350000
<b>210</b>	242.50000	0.951587163058	0.675365300402386	2.08039	0.105841445431462	0.0006641639168516150000
<b>270</b>	302.43690	0.949913885256	0.608839999052244	1.55650	0.082069511094135	0.0010559935784767700000
<b>330</b>	362.42210	0.949999723965	0.559815788131165	1.27178	0.066935976524076	0.0015753490671601500000
<b>390</b>	422.39880	0.950000126084	0.517576721663524	1.07287	0.056466611381372	0.0021936260396814000000
<b>450</b>	482.37035	0.950000425332	0.481054826145930	0.92699	0.048788291372031	0.0029115840999198900000
<b>510</b>	542.33715	0.950000294998	0.449140474781388	0.81534	0.042912620123921	0.0037279125705493400000
<b>570</b>	602.29950	0.949999834145	0.420994785267375	0.72710	0.038268563185204	0.0046411629003283300000
<b>630</b>	662.25766	0.949999601602	0.395973541409781	0.65556	0.034503269198201	0.0056498011701029100000
<b>690</b>	722.21187	0.950000381021	0.373573920032092	0.59636	0.031386987509892	0.0067522408221065600000
<b>750</b>	782.16225	0.949999555659	0.353381067173693	0.54651	0.028763737924662	0.0079462921999401600000

---

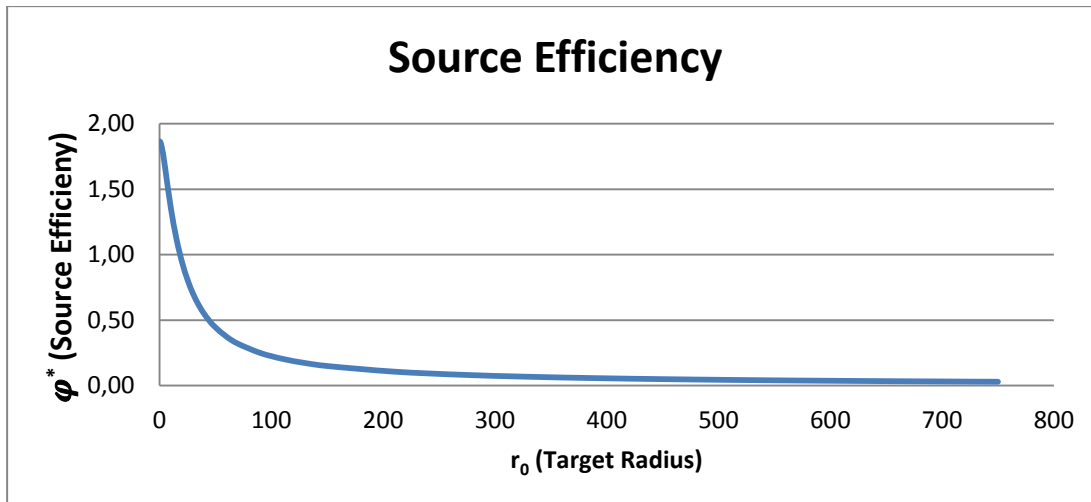


**Figure 7.1:** Target Radius and Source Efficiency Comparison.

While target radius increases, source efficiency decreases drastically, therefore the target radius must be kept as small as possible to maximize source efficiency. But since power level decreases as target radius decrease, an optimal value should be chosen that take bot power and source efficiency

## 7.2 Blanket Radius and Source Efficiency

To study the variaton of source efficiency with blanket radius  $R_0$  through numerical solution, values below are obtained keeping  $r_0$  at the constant value of 5.2 cm.

**Table 7.3:** Blanket Radius and Source Efficiency Comparison.

$r_0(cm)$	$R_0(cm)$	$k_{eff}$	$k_s$	$M_s$	$\phi^*$	$P(Watt)$
5.2	40	0.901962776	0.936698781	14.797484	1.608385947	0.0000000712800771
5.2	40.5	0.917346675	0.947303259	17.97650558	1.619690788	0.0000000866922427
5.2	41	0.932676906	0.95762368	22.59808492	1.63118973	0.0000001091005816
5.2	41.5	0.947951114	0.96766005	29.92150704	1.642891812	0.0000001446123228
5.2	42	0.963167037	0.977412636	43.272542	1.654807401	0.0000002093566545
5.2	42.5	0.978322511	0.986881913	75.23062837	1.666946363	0.0000003643408384
5.2	43	0.99341546	0.996068574	253.3606503	1.679320808	0.0000012282240051
5.2	43.1	0.996426371	0.997872067	468.9396269	1.681826369	0.0000022737294600
5.2	43.2	0.999434686	0.999664297	2977.827484	1.684359629	0.0000144412336397



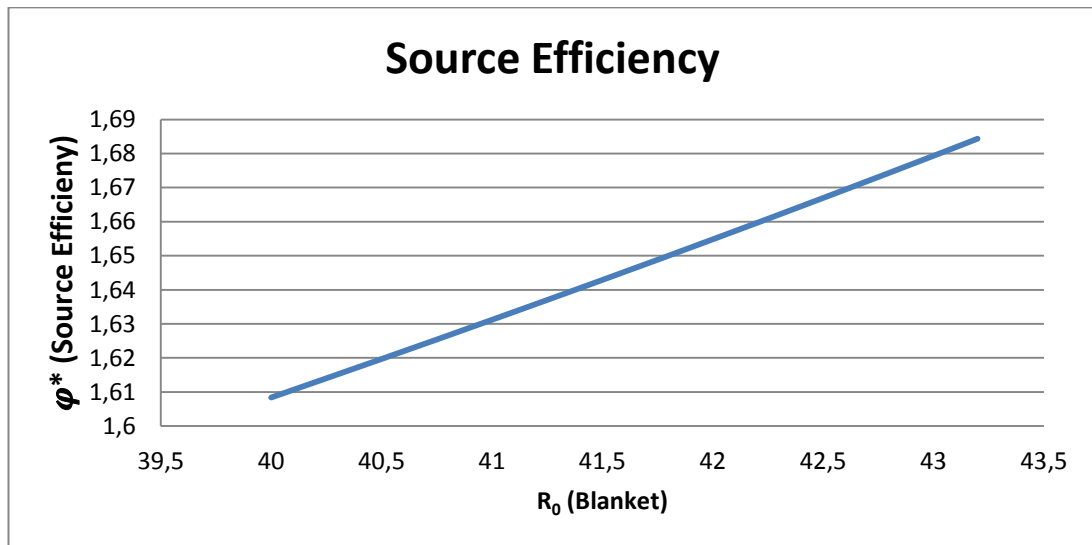


**Figure 7.2:** Blanket Radius and Source Efficiency Comparison.

While blanket radius increases, source efficiency increases almost linearly. This increase is expected due to the fact that increase in multiplying region radius, heightens the possibility of source neutrons to cause fission. But since  $k_{eff}$  must be kept around 0.95, there is a limitation on blanket radius.

### 7.3 Am-Pu Ratio Comparisons for An ADS

To demonstrate a fuel model for an ADS,  $\phi^*$  and other key parameters will be calculated for various ratios of Americium and Plutonium

**Table 7.4:** Elemental Densities.

Fuel Composition By Weight	Elemental Density (g/cm <sup>3</sup> )
<b>U (52.98%)</b>	5.83
<b>Pu(26.73%)</b>	2.94
<b>Am(9.01%)</b>	0.99
<b>O (11.27%)</b>	1.27

**Table 7.5:** Isotopic Compositions.

Elemental Composition (By Atom %)	U	Pu	Am
$^{235}\text{U}$	3.8		
$^{238}\text{U}$	96.2		
$^{238}\text{Pu}$		5	
$^{239}\text{Pu}$		38	
$^{240}\text{Pu}$		30	
$^{241}\text{Pu}$		13	
$^{242}\text{Pu}$		14	
$^{241}\text{Am}$			67
$^{243}\text{Am}$			33

To obtain percentage of an Americium and Plutonium mixed fuel

$$\frac{26.73}{(26.73 + 9.01)} = 0.7479 = 74.79\% \text{ Pu in (Pu - Am)}$$

$$\frac{9.01}{(26.73 + 9.01)} = 0.2521 = 25.21\% \text{ Am in (Pu - Am)}$$

For Elemental Composition

$$A^U = 0.038 * 235 + 0.962 * 238 = 237.89$$

$$A^{Pu} = 0.05 * 238 + 0.38 * 239 + 0.3 * 240 + 0.13 * 241 + 0.14 * 241 + 0.14 * 242 = 239.53$$

$$A^{Am} = 0.67 * 241 + 0.33 * 243 = 241.66$$

$$N^U = \frac{5.83 * 0.6022}{237.89} = 0.014766 \text{ b}^{-1}\text{cm}^{-1}$$

$$N^{Pu} = \frac{2.94 * 0.6022}{239.93} = 0.007379 \text{ b}^{-1}\text{cm}^{-1}$$

$$N^{Am} = \frac{0.99 * 0.6022}{241.86} = 0.0024676 \text{ b}^{-1}\text{cm}^{-1}$$

$$N^O = \frac{1.24 * 0.6022}{16} = 0.04667 \text{ b}^{-1}\text{cm}^{-1}$$

**Table 7.6:** Elemental Atom Densities.

Element	Densities ( $b^{-1}cm^{-1}$ )
$^{235}U$	$0.01476*0.038=5.61*10^{-4}$
$^{238}U$	$0.01476*0.962=1.42*10^{-2}$
$^{238}Pu$	$0.007379*0.05=3.69*10^{-4}$
$^{239}Pu$	$0.007379*0.38=2.80*10^{-3}$
$^{240}Pu$	$0.007379*0.3=2.21*10^{-3}$
$^{241}Pu$	$0.007379*0.13=9.59*10^{-4}$
$^{242}Pu$	$0.007379*0.14=1.03*10^{-3}$
$^{241}Am$	$0.002467*0.67=1.65*10^{-3}$
$^{243}Am$	$0.002467*0.33=8.14*10^{-4}$

For one group microscopic cross sections

**Table 7.7:** Elemental One Group Cross Sections.

Element	$\sigma_a(b)$	$\sigma_f(b)$	$\sigma_t(b)$
$^{235}U$	2.55	1.97	12.05
$^{238}U$	0.453	0.025	12.54
$^{238}Pu$	1.79	1.025	13.17
$^{239}Pu$	2.34	1.78	12.26
$^{240}Pu$	0.96	0.29	11.86
$^{241}Pu$	3.01	2.58	11.91
$^{242}Pu$	0.73	0.19	12.42
$^{241}Am$	2.15	0.19	12.30
$^{243}Am$	1.73	0.15	12.67
$^{16}O$	0.0006	0	3.5

Hence it is possible to calculate the macroscopic cross sections

$$\Sigma_{tr} = \sum_{i=1}^{i=10} ElementDensity(i) * \sigma_{tr}(i) = 0.468 cm^{-1}$$

$$D = \frac{1}{3\Sigma_{tr}} = 0.712 cm$$

$$\Sigma_a = \sum_{i=1}^{i=10} \text{ElementDensity}(i) * \sigma_a(i) = 0.0258 \text{ cm}^{-1}$$

$$\Sigma_f = \sum_{i=1}^{i=10} \text{ElementDensity}(i) * \sigma_f(i) = 0.0106 \text{ cm}^{-1}$$

For a mean  $\vartheta = 2.94$

$$\vartheta \Sigma_f = 2.94 * 0.0106 = 0.0312 \text{ cm}^{-1}$$

The target cross sections are as given in Table 7.8.

**Table 7.8:** Target and Fuel Cross Sections.

	$D(\text{cm})$	$\Sigma_a(\text{cm}^{-1})$	$\vartheta \Sigma_f(\text{cm}^{-1})$	$\Sigma_f(\text{cm}^{-1})$
Target	2.080	0.00178	0	0
Fuel	0.712	0.0258	0.0312	0.0106

$$k_{\infty} = \frac{\vartheta \Sigma_f}{\Sigma_a} = 1.2093$$

Now that  $k_{\infty}$  is obtained for the values of fuel and target, the parameters of  $k_s$  can be calculated for the values of

$$r_0 = 4.1745; R_0 = 32;$$

As:

$$k_s = 0.972375; k_{eff} = 0.951847; M_s = 35.1999; \varphi^* = 1.780732$$

The same calculations are made for different ratios of plutonium and americium mixes

**Table 7.9:** Nuclear Parameters for Pu/Am Mix Percentages.

$\%Pu/\%Am$	Target	80/20	75/25	70/30	65/35	60/40	55/45	50/50
$D$	2.080	0.71167	0.711542	0.711414	0.711286	0.711158	0.71103	0.710903
$\Sigma_a$	0.00178	0.0257226	0.0258394	0.0259563	0.0260731	0.0261899	0.026306	0.0264236
$\vartheta\Sigma_f$	0	0.0326164	0.0311643	0.0297122	0.02826	0.0268075	0.025355	0.0239036
$\Sigma_f$	0	0.011094	0.0106001	0.0101062	0.00961225	0.00911833	0.00862441	0.00813049
$k_\infty$	0	1.26801	1.20607	1.1447	1.08388	1.0236	0.96385	0.904633
$r_0$	4.1745	4.1745	4.1745	4.1745	4.1745	4.1745	4.1745	4.1745
$R_0$	0	32	32	32	32	32	32	32
$k_s$	0	0.998661	0.971088	0.940340	0.906704	0.870468	0.831917	0.791319
$k_{eff}$	0	0.997512	0.949746	0.902312	0.85521	0.808440	0.761994	0.715864
$M_s$	0	745.6777	33.587356	15.761737	9.718536	6.720120	4.949431	3.379200
$\varphi^*$	0	1.86009	1.777219	1.706426	1.645379	1.592339	1.545939	1.505096

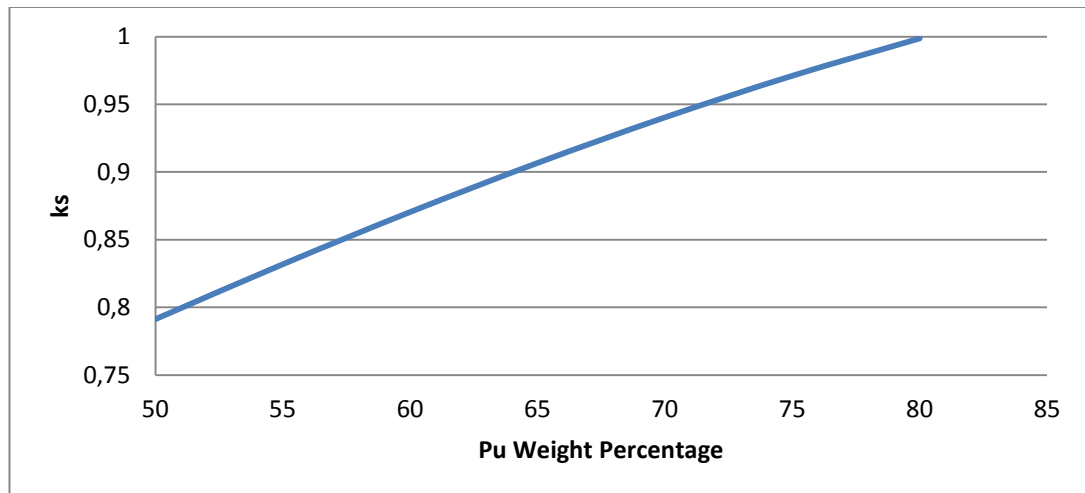


**Figure 7.3:**  $k_s$  vs plutonium weight percentage in Pu Am Fuel.

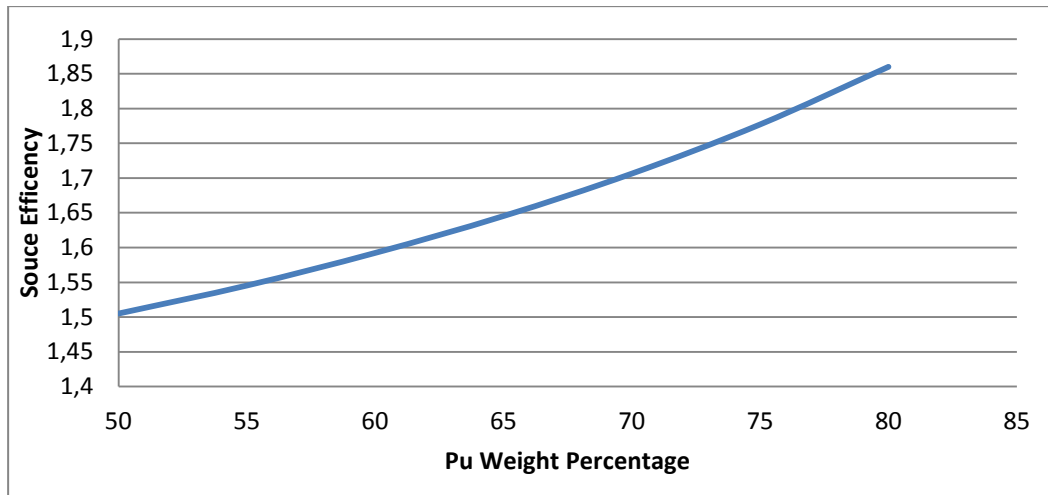


**Figure 7.4:**  $\varphi^*$  vs plutonium weight percentage in Pu Am Fuel.

With respect to these values that are obtained with plutonium ratio increasing, values for  $k_s$  and  $\varphi^*$  also increase, which is an expected result, since fission cross section of Pu isotopes are higher than Am isotopes.

## 8. CONCLUSION

One of the most important aspects of ADS design is the optimization of source efficiency, while keeping  $k_{eff}$  at a value (For example 0.95) that will both guarantee the sub criticality and continuous operation of the system.

In this thesis, the change of source efficiency has been observed with respect to various parameters. First, through analytical solutions of benchmark problems, source efficiency for four problems has been calculated. (Through MATHEMATICA)

Then, using the finite difference multi group diffusion code DIFSP (A.Özgener, 2012), results for the same benchmark problems have been obtained and compared to analytical results.

After confirmation of analytical and numerical results, the change in source efficiency with respect to material composition and geometry has been demonstrated

As such, while target radius increases, source efficiency decreases drastically, therefore the target radius must be kept as small as possible to maximize source efficiency in an ADS design

While as blanket radius increases, source efficiency increases almost linearly.

Also a benchmark americium and plutonium mixed fuel, with Americium ratio increasing, values of  $k_{eff}$ ,  $k_s$  and  $\varphi^*$  decrease fast. Therefore, in ADS fuel design the americium content must be kept within certain limits if the source efficiency is not to assume undesirably low values.





## REFERENCES

- Göksu, A.** (2010). *Multiplication Coefficients for accelerator-driven system* (M.Sc. dissertation). Institute of Energy, Istanbul Technical University.
- Seltborg, P.** (2005). *Source efficiency and high-energy neutronics in accelerator-driven systems* (Doctoral dissertation). Department of Nuclear and Reactor Physics, Royal Institute of Technology, Stockholm.
- Kobayashi, K.** (2005). The Rigorous Weight Function for Neutron Kinetics Equations of the Quasi-Static Method for Subcritical Systems. *Annals of Nuclear Energy*, 32, 763–766.
- Kobayashi, K., Nishihara, K.** (2000). Definition of Subcriticality Using the Importance Function for the Production of Fission Neutrons. *Nuclear Science and Engineering*, 136, 272-281.
- Nifenecker, H.** (2001). Basics of accelerator driven subcritical reactors. *Nuclear Instruments and Methods in Physics Research*, 463, 428–467.
- Shahbunder, H.** (2010). Subcritical Multiplication Factor and Source Efficiency in Accelerator-Driven System. *Annals of Nuclear Energy*, Vol. 37,9, 1214-1222.
- Shahbunder, H.** (2009). Experimental analysis for neutron multiplication by using reaction rate Distribution in accelerator-driven system. *Annals of Nuclear Energy*, Vol.37,4 592-597.
- Özgener, H.A.** (2012). Coarse Mesh Rebalance Acceleration of Power Iteration in Adjoint Diffusion Calculations. *Fusion Science And Technology*, Vol.61,15.
- Özgener, A.** (2009). Nuclear Waste Problem and Transmutation of Trans Uranium Elements. National Nuclear Science And Technology Meeting, 6-9 November.
- Özgener, B., Özgener, A.** (2014). Variational Acceleration of Fission Source Iteration for Subcritical, Source Driven Systems, PHYSOR-2014, 28 October.
- Url-1** <<http://www.psi.ch/bsq/spallation-target>>, date retrieved 01.12.2014.

- Url-2** <<https://www.oecd-nea.org>>, date retrieved 03.12.2014
- Eriksson, M.** (2005). *Accelerator-driven Systems: Safety and Kinetics* (Doctoral dissertation). Royal Institute of Technology, Stockholm.
- Wallenius, J.** (2003). Neutronic Aspects of Inert Matrix Fuels for Application in ADS, *Journal of Nuclear Materials*, 320, 142.
- Rubbia, C.** (1996). The Energy Amplifier, a Description for the non-Specialist CERN/AT Meeting, 29 September.
- Konings, R. J. M.** (2001). Advanced fuel cycles for accelerator-driven systems: fuel fabrication and reprocessing. 13th International Conference on Nuclear Engineering, 8 September.
- Wallenius, J., Pillon J.** (2001). N-15 Requirements for 2nd Stratum ADS Nitride Fuels, 9th International Topical Meeting on Nuclear Applications of Accelerators, 11-15 November.
- Lewins, J.** (1965). Importance, the adjoint function; the physical basis of the variational and perturbation theory in transport and diffusion problems. Pergamon Press Ltd, Headington Hill Hall Oxford.
- Duderstadt, J., Hamilton, L.** (1976). Nuclear Reactor Analysis. John Wiley&Sons Inc, Michigan USA.
- Bell, G., Glasstone, S.** (1970). Nuclear Reactor Theory. Litton Educational Publishing California.

## **CURRICULUM VITAE**



**Name Surname:** Ceyhun Yavuz

**Place and Date of Birth:** Istanbul 23.02.1983

**E-Mail:** ceyhunyavuz@gmail.com

### **EDUCATION:**

**B.Sc:** 10/2002-01/2008 Istanbul Technical University, Physics Engineering 2,25/4

**M.A:** 10/2008-08/2009 Istanbul Technical University, Executive MBA 3,3/4

### **PROFESSIONAL EXPERIENCE AND AWARDS:**

09/2014-Present ACM Software Development Company – Agile Coach

11/2011-09/2014 Cardtek – Project Manager

05/2008-09/2010 Yapı Kredi A.Ş. - P.O.S Product Management

08/2004-09/2004 Neutron Institute of Technology, Software Development Trainee